




Testing the deep-sea glacial disturbance hypothesis as a cause of low, present-day Norwegian Sea diversity and resulting steep latitudinal diversity gradient, using fossil records

Anna B. Jöst^{1,2}  | Huai-Hsuan M. Huang³ | Yuanyuan Hong^{4,5} | Chih-Lin Wei⁶  |
Henning A. Bauch⁷ | Benoit Thibodeau⁸ | Thomas M. Cronin⁹ | Hisayo Okahashi^{4,5} |
Moriaki Yasuhara^{4,5} 

¹Korea Institute of Ocean Science and Technology, Tropical and Subtropical Research Center, Jeju-si, Republic of Korea

²Department of Life Science, College of Natural Sciences, Hanyang University, Seoul, Republic of Korea

³Department of Geosciences, Princeton University, Princeton, New Jersey, USA

⁴School of Biological Sciences, Area of Ecology and Biodiversity, Swire Institute of Marine Science, Institute for Climate and Carbon Neutrality and Musketeers Foundation Institute of Data Science, The University of Hong Kong, Hong Kong SAR, China

⁵State Key Laboratory of Marine Pollution, City University of Hong Kong, Hong Kong SAR, China

⁶Institute of Oceanography, National Taiwan University, Taipei, Taiwan

⁷Alfred-Wegener-Institut Helmholtz Center for Polar and Ocean Research, c/o GEOMAR Helmholtz Centre for Ocean Research Kiel, Kiel, Germany

⁸Simon F.S. Li Marine Science Laboratory, School of Life Sciences, The Chinese University of Hong Kong, Hong Kong SAR, China

⁹Florence Bascom Geoscience Center, U.S. Geological Survey, Reston, Virginia, USA

Correspondence

Anna B. Jöst, Korea Institute of Ocean Science and Technology, Tropical and Subtropical Research Center, Iljudong-ro 2670, Gujwa-eup, Jeju-si, Jeju-do 63349, Republic of Korea.
Email: annajoest@outlook.com

Moriaki Yasuhara, School of Biological Sciences, The University of Hong Kong, Kadoorie Biological Science Building, Pokfulam Road, Hong Kong SAR, China.
Email: moriakiyasuhara@gmail.com

Funding information

U.S. Geological Survey Climate Research and Development Program; Peter Buck Postdoc Fellowship, Smithsonian Institution; Ministry of Science and ICT, South Korea, Grant/Award Number: 2019H1D3A1A01070922; the Ecology and Biodiversity Division Fund, Grant/Award Number: 5594129; Faculty of Science RAE Improvement Fund of the University of Hong Kong; Seed Funding Program for Basic Research of the University of Hong Kong, Grant/Award Number: 201210159043, 201411159017,

Abstract

Aim: Within the intensively-studied, well-documented latitudinal diversity gradient, the deep-sea biodiversity of the present-day Norwegian Sea stands out with its notably low diversity, constituting a steep latitudinal diversity gradient in the North Atlantic. The reason behind this has long been a topic of debate and speculation. Most prominently, it is explained by the deep-sea glacial disturbance hypothesis, which states that harsh environmental glacial conditions negatively impacted Norwegian Sea diversities, which have not yet fully recovered. Our aim is to empirically test this hypothesis. Specific research questions are: (1) Has deep-sea biodiversity been lower during glacials than during interglacials? (2) Was there any faunal shift at the Mid-Brunhes Event (MBE) when the mode of glacial–interglacial climatic change was altered?

Location: Norwegian Sea, deep sea (1819–2800 m), coring sites MD992277, PS1243, and M23352.

Time period: 620.7–1.4 ka (Middle Pleistocene–Late Holocene).

Taxa studied: Ostracoda (Crustacea).

Methods: We empirically test the deep-sea glacial disturbance hypothesis by investigating whether diversity in glacial periods is consistently lower than diversity in interglacial periods. Additionally, we apply comparative analyses to determine

This is an open access article under the terms of the [Creative Commons Attribution-NonCommercial-NoDerivs](https://creativecommons.org/licenses/by-nc-nd/4.0/) License, which permits use and distribution in any medium, provided the original work is properly cited, the use is non-commercial and no modifications or adaptations are made.

© 2024 The Authors. *Global Ecology and Biogeography* published by John Wiley & Sons Ltd.

201511159075, 202011159122 and 2202100581; the Research Grants Council of the Hong Kong Special Administrative Region, China, Grant/Award Number: HKU 17301818, HKU 17311316 and RFS2223-7502; the Korea Institute of Ocean Science and Technology, Grant/Award Number: PO01471 and PEA0205

Handling Editor: Adam Tomasovych

a potential faunal shift at the MBE, a Pleistocene event describing a fundamental shift in global climate.

Results: The deep Norwegian Sea diversity was not lower during glacial periods compared to interglacial periods. Holocene diversity was exceedingly lower than that of the last glacial period. Faunal composition changed substantially between pre- and post-MBE.

Main conclusions: These results reject the glacial disturbance hypothesis, since the low glacial diversity is the important precondition here. The present-day-style deep Norwegian Sea ecosystem was established by the MBE, more specifically by MBE-induced changes in global climate, which has led to more dynamic post-MBE conditions. In a broader context, this implies that the MBE has played an important role in the establishment of the modern polar deep-sea ecosystem and biodiversity in general.

KEYWORDS

deep-sea diversity, faunal turnover, macroecological patterns, Mid-Brunhes Event, North Atlantic, Ostracoda

1 | INTRODUCTION

Macroecological patterns, such as the classic deep-sea biodiversity patterns, namely the latitudinal diversity gradient and the depth diversity gradient, were first discovered in the North Atlantic Ocean (Ramirez-Llodra et al., 2010; Rex & Etter, 2010). The deep-sea latitudinal diversity gradient, which defines a decrease in deep-sea species diversity with increasing latitude, has since been intensively studied in that area (Corliss et al., 2009; Jöst et al., 2019; Lamshead et al., 2000; Rex et al., 1993, 2000; Tittensor et al., 2011; Yasuhara, Okahashi, & Cronin, 2009). The Norwegian Sea, which is situated within the North Atlantic Gateway (Figure 1; also see Jöst et al., 2019), is characterized by a low deep-sea biodiversity that constitutes an important part of the North Atlantic deep-sea latitudinal diversity gradient. Notably low benthic alpha diversities in the Norwegian Sea have been reported across many taxonomic groups, for example in gastropods, bivalves and isopods (Rex et al., 1993, 2000; Svavarsson, 1997; Svavarsson et al., 1993), amphipods (Dahl, 1979), nematodes (Lamshead et al., 2000), foraminiferans (Culver & Buzas, 2000) and ostracods (Jöst et al., 2019; Yasuhara, Hunt, et al., 2009; Yasuhara, Hunt, Dowsett, et al., 2012), resulting in a low regional benthic diversity. Many researchers attribute this low Norwegian Sea benthic deep-sea biodiversity to, at least in part, “Quaternary glaciation”. As summarized in Rex et al. (1997) and Culver and Buzas (2000), it is often implied that a glacial disturbance (or the effect of glaciation: Rex et al., 1993) had, at the time, negatively affected the Norwegian Sea deep-sea benthic diversity to an extent that it has not yet fully recovered from the disturbance. However, there are two uncertainties in their arguments, which entail the exact meaning of (1) “Quaternary glaciation”, and (2) “glacial disturbance”. Some papers specify the time of the disturbance, estimating it to have occurred during the last glacial period (Svavarsson, 1997), whereas others generalize by saying “Quaternary glaciation”, or “Pleistocene glaciations”, etc. (Bodil et al., 2011;

Lamshead et al., 2000; Rex et al., 1993, 1997, 2005). Hence, the meaning of “Quaternary glaciation” should be either the last glacial period (a.k.a. last ice age, 70,000 to 11,700 years BP) or multiple glacial periods during the Pleistocene. The term “glacial disturbance” may imply that harsh environmental glacial conditions eradicated the deep-sea fauna and negatively affected the deep-sea diversity in the Norwegian Sea at that time, although the responsible environmental parameter(s) has (have) never been specified (Bodil et al., 2011; Culver & Buzas, 2000; Rex et al., 1993, 2005; Stuart & Rex, 2009).

Paleobiology uses microfossils in sediment cores as a tool to reconstruct past ecosystem and biodiversity dynamics with high time resolution and accuracy, also known as “time machine biology” (Yasuhara, 2018; Yasuhara et al., 2015, 2020; Yasuhara & Deutsch, 2022). Marine ostracods (Crustacea, Ostracoda, Podocopida) are a large group of small benthic (i.e. meiobenthic) invertebrates, and are the best represented marine metazoans, ecdysozoans and arthropods in sediment core-based fossil research (Schellenberg, 2007; Yasuhara et al., 2022; Yasuhara & Cronin, 2008). Their well-calcified fossilized remains represent a major part of their body (carapace) and are preserved in small-volume samples from sediment cores abundantly enough for rigorous statistical analyses of their diversity and faunal composition. This is in contrast to most, if not all, other metazoan invertebrates, as they either have limited fossilization potential (due to a lack of hard parts) or low abundance (because of their large size). Thus, ostracods are an excellent model system representing, especially, small marine invertebrates (Chiu et al., 2020) that account for about two thirds of marine biodiversity (Leray & Knowlton, 2015).

The Mid-Brunhes Event (MBE) refers to a major shift in Pleistocene climate (at ~430–350 ka) that marks the final stage of the climate transition from low-amplitude to high-amplitude glacial–interglacial climatic variability (Cronin et al., 2010, 2017; DeNinno et al., 2015; Yin & Berger, 2010). This fundamental shift in climate

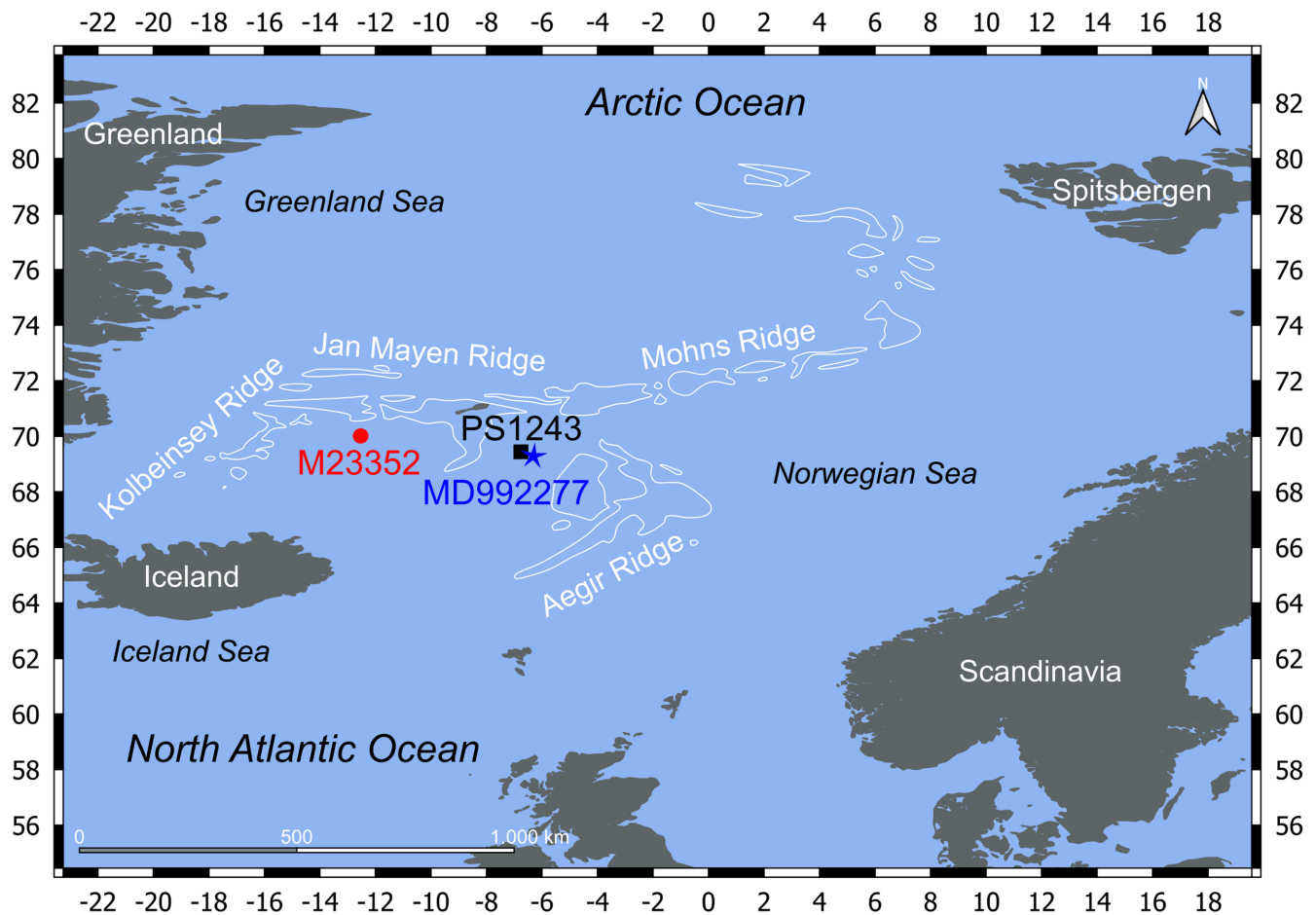


FIGURE 1 Locality map depicting the three coring sites within the Nordic Seas and the Jan Mayen fracture zone. Ridges: white lines based on 1000, 2000, and 3500m depth contour, respectively. Coring location of studied core is indicated by blue star (MD992277); coring locations of referenced cores indicated by red dot (M23352) and black square (PS1243), respectively. MD992277: Piston core (Labeyrie et al., 1999); M23352: Kasten core M23352(-3) (Hirschleber et al., 1988), PS1243: Composite core of PS1243(-1) and PS1243(-2) (Augstein et al., 1984).

involves large-scale changes in ice shelf development, sea ice volume, global ocean circulation and potentially marginal marine systems that are sensitive to changes in climate (Huang et al., 2018). From analyses of microfossils in deep-sea sediment cores, major faunal shifts and extinctions have recently been reported across the MBE in various places (Cronin et al., 2014, 2017; DeNinno et al., 2015; Hayward et al., 2007, 2012; Huang et al., 2018, 2019; Polyak et al., 2013; Zarikian et al., 2022). If “Quaternary glaciation” plays a role in the deep Norwegian Sea biodiversity, a shift in the mode of glacial–interglacial climatic variability may affect it to a certain degree.

The above-mentioned glacial disturbance hypothesis as reason for the low deep-sea benthic biodiversity in the present-day Norwegian Sea has never been rigorously tested. Here, we empirically test this hypothesis by using an alpha-scale diversity dataset of fossil ostracods in the sediment core MD992277 and published ostracod census data from two additional sediment cores (M23352 and PS1243) from the deep Norwegian Sea. Specific research questions are: (1) Was the benthic deep-sea biodiversity lower during glacials than during interglacials? (2) Was there any faunal shift at the MBE when the mode of glacial–interglacial climatic change was altered? Our paleobiological result shows that the actual long-term benthic deep-sea biodiversity

trend in the Norwegian Sea was not consistent with the trend presumed by the glacial disturbance hypothesis, thus rejecting this hypothesis. Benthic deep-sea biodiversity in the glacial Norwegian Sea was not lower than that of interglacial periods, including the present day. Especially the Holocene diversity is much higher than that of the last glacial period, therefore, the present-day deep Norwegian Sea benthic diversity cannot be in the middle of its recovery process. This result highlights the importance of paleobiological data for empirically testing hypotheses to explain present-day diversity patterns that often involve speculations about historical processes.

2 | METHODS

2.1 | Coring location and sample treatment

Although the sediment of each core was sieved into varying size fractions, ultimately, all ostracod specimens were picked from sediment of $>125\mu\text{m}$, that is mesh size effect can be disregarded.

Piston core MD992277 (in the following referred to as just MD992277) was obtained with a Calypso Piston Corer onboard

the French R/V *Marion-Dufresne* in 1999 as part of the IMAGES program (02.08.1999; 5th cruise, leg 3: Reykjavik, Iceland to Tromsø, Norway; Labeyrie et al., 1999). The coring site was the western Norwegian Basin at the eastern slope of the Iceland Plateau, along the eastern flank of the Jan Mayen Ridge at 2800 m water depth (69°15.01'N, 06°19.75'W) (Figure 1; Table S1, given as Appendix 1 in Online Supplement S1). A total length of 33.66 m of sediment core with a diameter of 12 cm was retrieved. The core was cut lengthwise, in half. Only one of the half-cores was sampled; the other one was archived. The sampling half-core was cut into 1-cm sediment samples, every 1, or alternating 2 and 3 cm, depending on core section. Roughly $\frac{3}{4}$ of the half-core was sampled. The sediment volume was $\sim 27 \text{ cm}^3$ per each 1-cm sediment layer. This study investigated 1-cm thick sediment samples of a 7.11 m long core segment (10.45–17.56 m original core depth, equivalent to 620.7–361.6 ka; Table S1, given as Appendix 1 in Online Supplement S1). A total of 432 samples was studied for ostracods (see raw census file supplied as S2). Each sample was split into 2 and 3 grain size fractions, respectively, depending on core section. The core section of this study contained 397 samples that were split into 3 grain size fractions: 125–250, 250–500, and $>500 \mu\text{m}$, and 35 samples that were split into 2 grain size fractions: 150–500 and $>500 \mu\text{m}$. Fractions were merged for ostracod census data to get complete samples of a specific age. Effectively, all sediment of $>125 \mu\text{m}$ was picked for ostracods. Ostracod specimens were picked, sorted, and identified at the University of Hong Kong (HKSAR) and Hanyang University (ROK). Taxonomic identification was based mainly on Sylvester-Bradley (1973), Whatley and Coles (1987), Cronin (1989), Coles et al. (1994), Whatley et al. (1996, 1998), Stepanova et al. (2004), Wood (2005), Jellinek et al. (2006), Yasuhara, Okahashi, and Cronin (2009), Yasuhara et al. (2013), Yasuhara et al. (2014), Yasuhara and Okahashi (2014, 2015), Gemery et al. (2015).

Kasten core M23352(-3) (in the following referred to as simply M23352) was obtained with a Kastenlot Corer onboard the German R/V *Meteor* in 1988 as part of the *Meteor* 7 expedition (M7; Hirschleber et al., 1988). The coring site was the western part of the southern Norwegian Basin at the eastern slope of the Iceland Plateau, along the northwestern flank of the Jan Mayen Ridge at a water depth of 1819 m (70°00.4'N, 12°25.8'W) (Figure 1; Table S1, given as Appendix 1 in Online Supplement S1). The sampling half-core was cut into 1-cm sediment samples, every 1–3 cm, from the uppermost layer down to 350 cm, whereas the uppermost layers were spliced together with an additional trigger boxcore to ensure undisturbed top sediment layers (Didié & Bauch, 2002). Sediment samples were divided into grain size fractions of 125–250, 250–500, and $>500 \mu\text{m}$. Ostracods were picked, counted and identified from these separate size fractions, although the results were later merged for ostracod census data to get complete samples of a specific age. Effectively, all sediment of $>125 \mu\text{m}$ was picked for ostracods. This study included 143 sediment samples of 1 cm thickness of a 3.48 m-long core segment (2–350 cm original core depth, equivalent to 194.5–4.2 ka), yielding a total of 26,138 ostracod valves (Figure 2; Table S1, given

as Appendix 1 in Online Supplement S1). Ostracod census data (S2) and the age model (Figure 2) are from Didié et al. (2002).

Gravity core PS1243(-1) was obtained with a Gravity Corer onboard the German R/V *Polarstern* in 1984 as part of the Arktis 2 program (ARK II/5) together with the trigger boxcore PS1243(-2) obtained with a Box Corer (Augstein et al., 1984). The coring site was the Iceland Sea at the eastern slope of the Iceland Plateau at 2710 m [PS1243(-1)] and at 2716 m [PS1243(-2)] water depths, respectively, along the eastern flank of the Jan Mayen Ridge [PS1243(-1) at 69°22.3'N, 06°32.1'W; PS1243(-2) at 69°22.5'N, 06°32.4'W] (Kandiano, 2003) (Figure 1; Table S1, given as Appendix 1 in Online Supplement S1). In case of the main core PS1243(-1), fifty-five sediment samples of 1 cm thickness of a roughly 7.47 m-long core segment (8–755 cm original core depth, equivalent to 339.9–2.7 ka) treated with a sieve of $>125 \mu\text{m}$ mesh size, yielding a total of 2853 ostracod valves, were included in this data set (Appendix 1 in Online Supplement S1). The core had a diameter of 10 cm and the sampling half-core was sampled every 1 cm throughout. For low-specimen-count samples within the uppermost 50 cm of sea floor sediment, additional sediment from the trigger boxcore was used to increase specimen counts to >10 valves. From this additional boxcore PS1243(-2), six sediment samples of 1 cm thickness of a 37 cm core segment (1.5–38.5 cm original core depth, equivalent to 10.9–1.4 ka), yielding a total of 119 ostracod valves, were included in this data set (Appendix 1 in Online Supplement S1). The boxcore had a size of $50 \times 50 \times 50 \text{ cm}$ and was sampled every 2 cm, with additional sampling by 10 mL syringes for accumulation rate calculations (Bauch, Struck, & Thiede, 2001). Sediment samples were sieved into 63–125 and $>125 \mu\text{m}$ size fractions for foraminiferal assemblages, whereas the smaller size fraction was not used for picking ostracods. Ostracod census data and the age model for composite core PS1243 [i.e. merged cores PS1243(-1) and (-2); in the following referred to as simply PS1243] are from Cronin et al. (2002) and Bauch, Struck, and Thiede (2001), respectively. All sediment of $>125 \mu\text{m}$ was picked for ostracods. A total of 3072 ostracod valves from PS1243 were included in this study (S2).

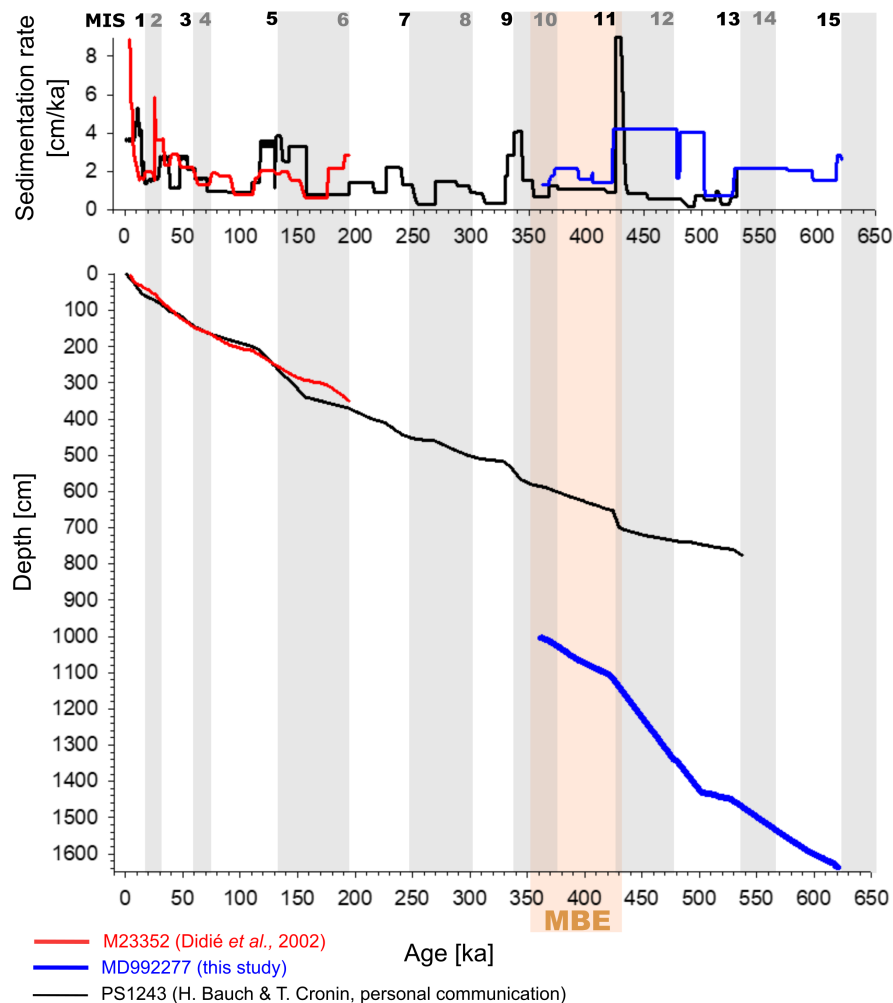
2.2 | Chronology

Age models (i.e. age/depth relationships) and linear sedimentation rates of cores M23352 (from the northwestern flank of the Jan Mayen Ridge) and PS1243 and MD992277 (from the eastern flank of the Jan Mayen Ridge) are plotted in Figure 2.

2.2.1 | For the core MD992277

The chronology applied was published in Helmke, Bauch, and Erlenkeuser (2003), Helmke, Bauch, and Mazaud (2003). Magnetic inclination, sediment density, lightness and carbonate content were used as sedimentary clocks. The adopted age scheme retrieved from these sedimentological parameters was calibrated and standardized

FIGURE 2 Age models and sedimentation rate through time. Black lines refer to PS1243 data, red to M23352 data, and blue depicts core MD992277. MIS: Marine Isotope Stage; grey highlighted areas indicate glacial periods (even MIS); Mid-Brunhes Event indicated by bisque colour bar from 350 to 430 ka (according to Yin and Berger [2010] and Cronin et al. [2017]). Top: sedimentation rates through time given in cm sediment per ka based on raw data. Bottom: age models depicted as depth/age relationship line graph.



by correlation to the benchmark $\delta^{18}\text{O}$ chronology records of SPECMAP by linear interpolation between the points of correlation. Surface layers (uppermost 50 cm of sediment) were correlated with PS1243 due to corer-related disturbance in sediment layers (Helmke, Bauch, & Mazaud, 2003). Well-documented characteristic trends in sediment density, lightness, carbonate content, foraminiferal fluxes, and the amount of coarse lithic fraction in respect to Pleistocene Nordic Sea sediments, were used to identify cold and warm marine isotope stages (MIS) (see Bauch & Kandiano, 2007; Elliot et al., 1998; Helmke, Bauch, & Mazaud, 2003). MIS boundaries were set according to Lisiecki and Raymo (2005). The core section used in this study was determined to span from the beginning of MIS 15 (620.7 ka) to the beginning of MIS 10 (361.6 ka) (see Table S1, given as Appendix 1 in Online Supplement S1). Further details regarding core chronology are given in Appendix 2 in Online Supplement S1.

2.2.2 | For the core M23352

The chronology applied was published in Bauch and Helmke (1999), Didié and Bauch (2002), and Helmke and Bauch (2003). Foraminiferal oxygen isotope analysis was based on planktonic and benthic species, whereas for isotope analyses on ostracods, specimens of two

genera with near-continuous time-record were used. Overall, the age model is based on the synchronization of planktic foraminiferal $\delta^{18}\text{O}$ and the sediment lightness record to the standard SPECMAP chronology after applying a smooth filter with a 14-point least squares running average (Helmke & Bauch, 2003). This study includes M23352 sediments between 194.5–4.2 ka (Table S1, given as Appendix 1 in Online Supplement S1). Further details regarding core chronology are given in Appendix 2 in Online Supplement S1.

2.2.3 | For the core PS1243

The chronology applied was partially based on published records in Bauch (1997), Bauch and Helmke (1999), and Bauch et al. (2000). Planktic foraminiferal $\delta^{18}\text{O}$ records were correlated to carbonate content to establish the downcore positions of MIS (Kandiano et al., 2016). Additionally, the reflectance of sediments was measured across glacial and interglacial sections of the core and compared to the results of other Norwegian Sea cores, including M23352 (Bauch & Helmke, 1999). The adopted age scheme was calibrated and standardized by correlation to the benchmark $\delta^{18}\text{O}$ chronology records of SPECMAP (Bauch et al., 2000). The age/depth curve correlates well with the age/depth curve from the overlapping

age sections of core M23352, signifying comparable sedimentation rates, and therefore supporting the comparability and compatibility of both cores (Figure 2). This study includes PS1243 sediments between 339.9–1.4 ka (Table S1, given as Appendix 1 in Online Supplement S1). Further details regarding core chronology are given in Appendix 2 in Online Supplement S1.

2.3 | Data analyses

MD992277 dataset consists of 15,293 ostracod specimens collected from 297 ostracod-bearing sediment samples spanning 620.7–361.6 ka (Table S1, given as Appendix 1 in Online Supplement S1). PS1243 yielded 3072 ostracod specimens collected from 61 sediment samples corresponding to ~532.1–1.23 ka (Table S1, given as Appendix 1 in Online Supplement S1; census file, given as S2). M23352 contained 26,019 ostracod specimens obtained from 143 sediment samples from between 194.5–4.2 ka (all post-MBE; Table 1; Figure 2; Appendix 1). Allochthonous taxa, that is deposited on site by down-slope transport or ice-rafting events (known shallow-marine species; see Table S2, given as Appendix 3 in Online Supplement S1 for MD992277 and M23352 data), as well as specimens without, at least, genus level identification were omitted from analyses.

To determine the general trend of abundance fluctuations over time, autochthonous ostracod specimen counts (i.e. raw counts) of the three cores were plotted along the total age scale of ~640–0 ka (Figure 3). Similarly, autochthonous ostracod diversity was plotted

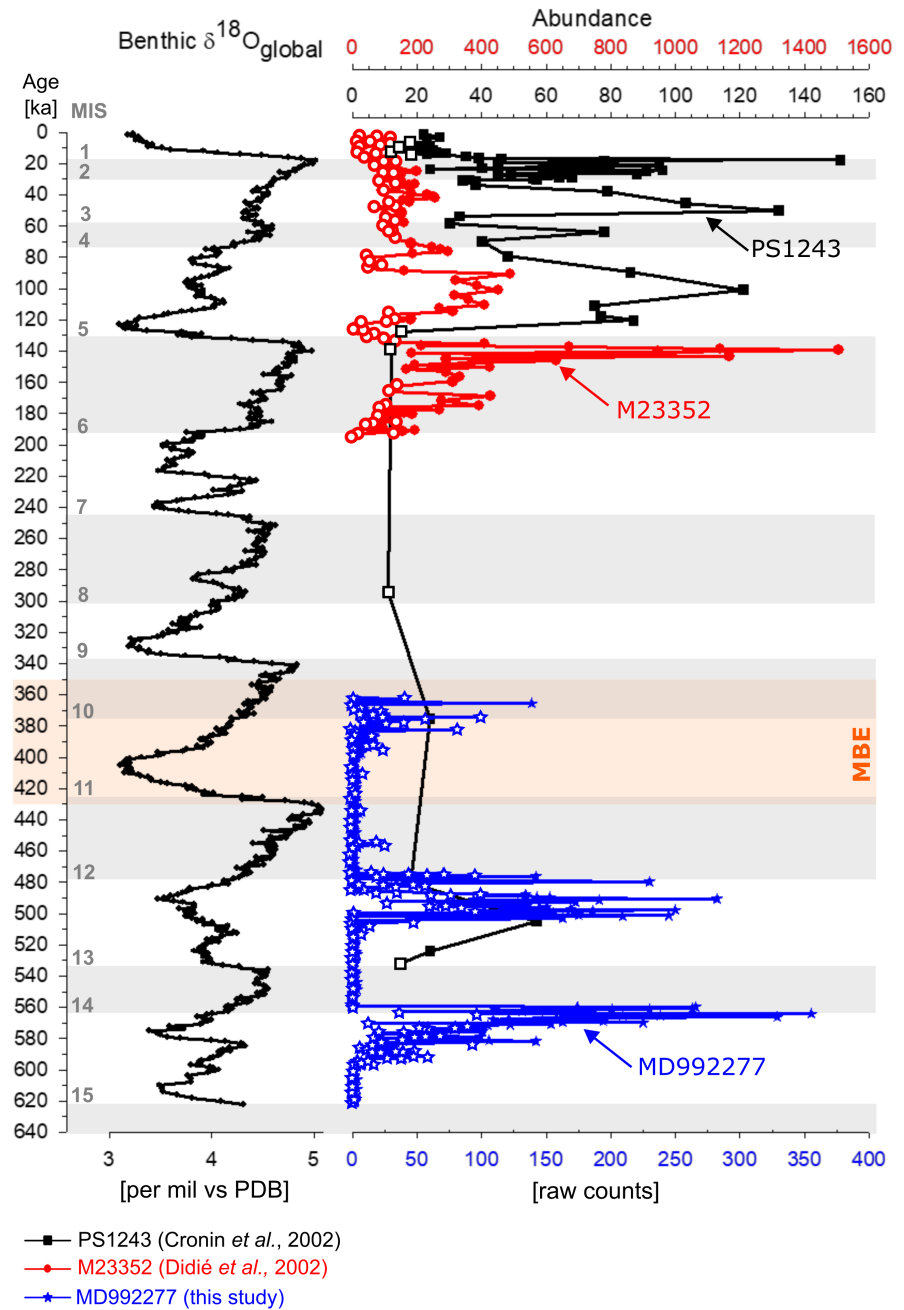
as function of age along the benthic $\delta^{18}\text{O}$ paleoclimatic trend (Figure 4). Ostracod diversity was given as Hill number, a measure of the effective number of species in a hypothetical community (Chao et al., 2014). The Hill number (qD) is calculated based on the q th power sum of the relative species abundance; therefore, the q value determines its sensitivity to the relative species abundance. In this study, we employed the three most commonly adopted Hill numbers: $q=0$ (0D or species richness), $q=1$ (1D or Shannon diversity), and $q=2$ (2D or Simpson diversity) to evaluate the species richness and diversity emphasis on abundant (i.e. 1D) and highly abundant (i.e. 2D) species. Alpha (Figure 5, upper panel), as well as gamma diversities (Figure 5, lower panel) were calculated, while we consider pooled diversity (MISs and pre-, during- and post-MBE) as a measure for a less biased diversity by abundance and sedimentation rate. Gamma diversity (i.e. pooled diversity of each bin, as opposed to average of each individual sample per, e.g. MIS) was used to investigate glacial versus interglacial and pre- versus post-MBE trends (Figure 5 and Figure S1, given as Appendix 4 in Online Supplement S1). To standardize the sampling efforts, we performed coverage-based rarefaction and extrapolation (sample coverage=85% for alpha diversity, and 99% for gamma diversity) using 1000 bootstrap resampling (Chao et al., 2020). Both the observed (i.e. unstandardized) and estimated Hill numbers (i.e. standardized to 85% sample coverage) are reported. As result, 11 samples (~2.2% of total) were removed before analysis due to low sample coverage (<85%). PERMANOVA (Permutational Multivariate Analysis of Variance) was performed

Taxon	Before MBE (N=219)		After MBE (N=198)	
	Relative abundance (%)		Relative abundance (%)	
	Average	Standard deviation	Average	Standard deviation
Allochthonous	1.80	8.04	5.27	6.3
<i>Cytheropteron</i>	13.73	18.57	30.15	22.45
<i>Eucythere</i>	5.86	13.46	1.38	3.25
<i>Henryhowella</i>	7.3	7.41	31.70	26.21
<i>Krithe</i> (all)	68.97	31.03	40.48	20.30
<i>Krithe hunti</i>	62.44	32.45	16.27	25.32
<i>Krithe minima</i>	0.83	7.54	18.92	19.94
<i>Paracytherois</i>	2.33	9.35	0.37	1.13
<i>Polycyope</i>	3.11	13.00	4.39	10.32
<i>Propontocypris</i>	0.006	0.87	0.06	0.43
<i>Pseudocythere</i>	1.44	10.21	2.38	5.36
	Raw count per sample		Raw count per sample	
	Average	Standard deviation	Average	Standard deviation
Total abundance	67	90	143	184

Note: Average relative abundance values of ostracod taxa and their standard deviations within the total pre-MBE and post-MBE assemblages of Norwegian Sea cores MD992277 (N=213), M23352 (N=143), and PS1243 (N=61). Pre-MBE sample size is N=219 (213 from MD992277; 6 from PS1243); post-MBE sample size is N=198 (143 from M23352; 55 from PS1243). Taxa given in bold are subject to bias in taxonomic handling, that is absent in M23352 after the MBE, hence sample size for calculations is lower (N=55).

TABLE 1 Comparison of relative abundances before and after the Mid-Bruhnes Event.

FIGURE 3 Abundance comparison to global benthic $\delta^{18}\text{O}$ changes from ~630 ka to present day. Black squares denote ostracod data obtained from PS1243 (Cronin et al., 2002); red dots denote ostracod data obtained from M23352 (Didié et al., 2002); blue stars denote ostracod data obtained from MD992277 (this study). Low abundance samples omitted from the nMDS analysis are indicated by open symbols. Different scales for x-axes applied: MD992277 data plotted along blue scale at the bottom, M23352 (red scale) and PS1243 (black scale) data plotted along scales shown at the top. MIS: Marine Isotope Stage; grey highlighted areas indicate glacial periods (even MIS); white highlighted areas indicate interglacial periods (odd MIS); Mid-Brunhes Event indicated by bisque colour bar from 350 to 430 ka (according to Yin and Berger [2010] and Cronin et al. [2017]). Abundance given in total raw counts.



to quantify comparisons of pre- and post-MBE diversity. Barren samples were removed prior to PERMANOVA computation. The 84 ostracod-bearing MBE samples (350–430 ka) were not included (Table S3, given as Appendix 5 in Online Supplement S1), as PERMANOVA works better for balanced designs (Anderson & Walsh, 2013) and our focus lies on the differences before and after the MBE, rather than on the MBE itself. PERMANOVA was computed with the R package “vegan” (Oksanen et al., 2018). The diversity calculations were computed with the R package “iNEXT” (Hsieh et al., 2020). Core localities were mapped with the software QGIS (version 3.16.8 Hannover; 1989, 1991, Free Software Foundation, Inc.). Continent shape files were acquired through open sources at <https://www.igismap.com>, country specific

shape files through https://gadm.org/download_country_v3.html. Faunal diagrams were generated with the software SigmaPlot (version 10.0; 2006, Systat Software, Inc.) and edited with vector graphics software Inkscape (0.92.1 version 3; 2007, Free Software Foundation, Inc.). Non-metric multidimensional scaling (nMDS) was used to understand the relationships among samples and taxonomic variables, generating a two-dimensional configuration of the faunal assemblages, while preserving their ranks of differences (Borcard et al., 2011; Legendre & Legendre, 2012). To reduce bias caused by the differences in numbers of samples available for the three cores, nMDS was run using uneven specimen cut-off thresholds, so that each core has roughly the same number of samples (i.e. around 50). For PS1243, $a \geq 20$ specimen-cut-off

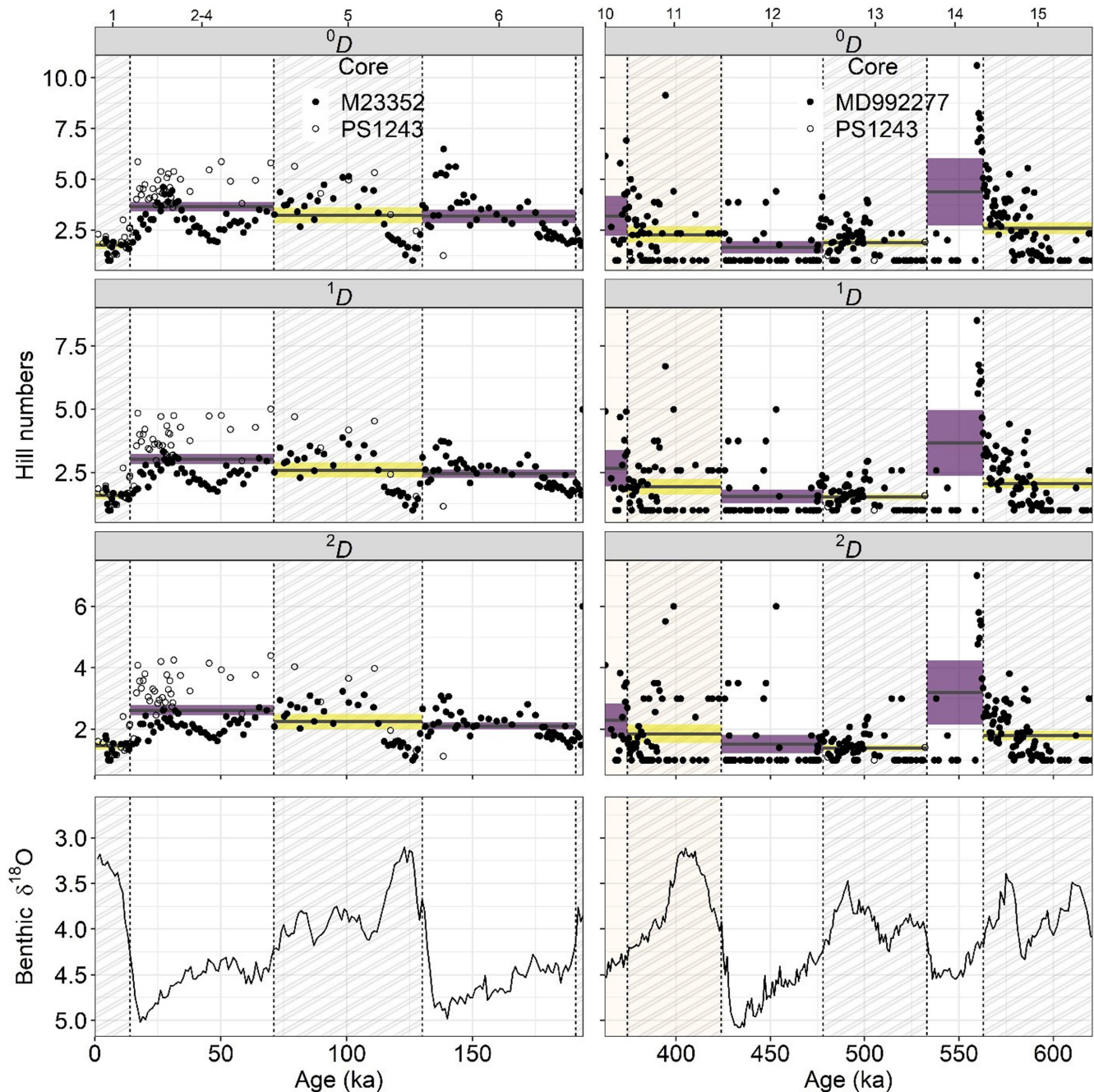


FIGURE 4 Estimated Hill numbers (qD) of order $q=0$ (0D), $q=1$ (1D) and $q=2$ (2D) based on 85% sample coverage as function of age. The striped rectangles indicate interglacial periods. The bisque colour background shows the MBE period (~350–430 ka). The top x-axis shows Marine Isotope Stages. The horizontal lines show the mean and the shaded area show 95% confidence interval (mean \pm standard error * 1.96). Note that black dots for the left panels indicate the M23352 samples and those for the right panels indicate MD992277 samples.

was applied, resulting in 52 samples (9 low-count samples omitted); for M23352, $a \geq 150$ specimen-cut-off was applied, resulting in 58 samples (85 low-count samples omitted); and for MD992277, $a \geq 100$ specimen-cut-off was applied, resulting in 58 samples (374 low-count samples omitted). Omitted samples are indicated by open symbols in Figure 3. We applied Bray–Curtis dissimilarity on relative abundances of the allochthonous taxa and all 16 genera that are present in this subset for the nMDS. The analysis was done using the R package “vegan” (Oksanen et al., 2018).

3 | RESULTS

3.1 | Diversity

Diversity as calculated by Hill numbers (0D , 1D , 2D) (Chao et al., 2014) shows substantial glacial–interglacial and shorter time-scale variations (Figure 4). Generally, glacial alpha diversity tends to be higher than interglacial alpha diversity, especially in MISs 2–4, 10 and 14 (at least for $q=0$, i.e. rare species diversity)

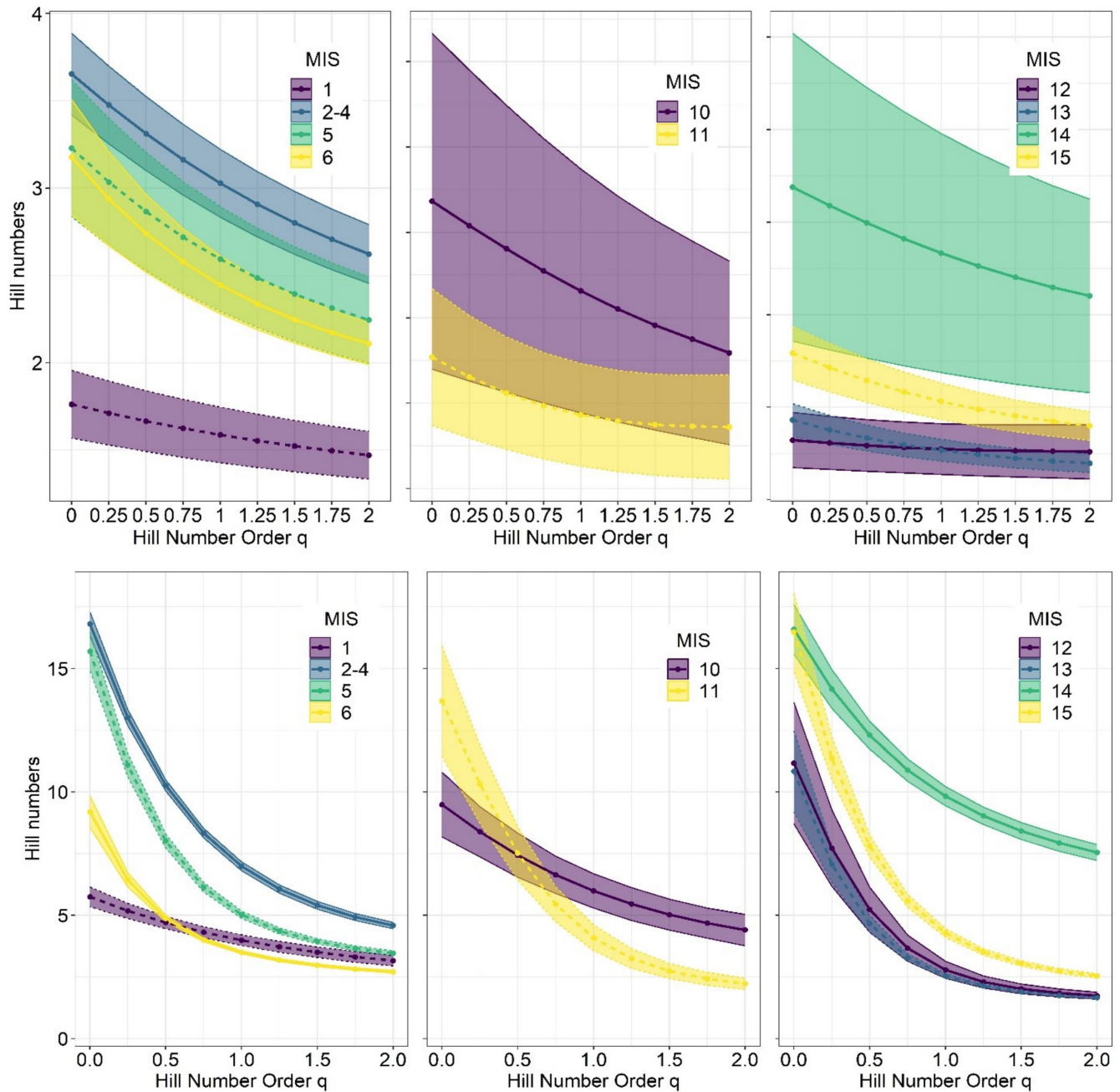


FIGURE 5 Alpha and gamma diversity by Marine Isotope Stage. Top: Alpha diversity. Mean Hill numbers based on 85% sample coverage as function of order q . The curves show the mean Hill numbers (i.e. mean alpha diversity) and the shaded area shows the 95% confidence interval (mean \pm standard error \times 1.96). Bottom: Gamma diversity. The curves show the pooled Hill numbers (i.e. gamma diversity) based on 99% sample coverage. Non-overlap of shaded areas indicates significant difference in diversity. Colours indicate MIS stages as shown in the legends on the figures. Interglacial MIS denoted by dashed lines (pre-MBE MIS 13, 15; MBE MIS 11; post-MBE MIS 1, 5), while glacial MIS denoted by solid lines (pre-MBE MIS 14, 12; MBE MIS 10; post-MBE MIS 6, 2-4).

(Figure 5, upper panel). Glacial gamma diversity also tends to be higher than interglacial gamma diversity, especially in MISs 2-4, and 14 (Figure 5, lower panel). Post-MBE diversity tends to be higher than pre-MBE diversity in alpha diversity, but it is the opposite in gamma diversity (Figure S1, given as Appendix 4 in Online Supplement S1).

3.2 | Relative and total abundance

Looking at the relative abundance data of ostracod taxa from the three cores, the following patterns are revealed:

Prior to the MBE, *Eucythere*, *Krithe* and *Paracytherois* show higher mean relative abundances when compared to their

post-MBE abundance rates, although the respective standard deviations are substantial (Table 1). On the contrary, *Cytheropteron*, *Henryhowella* and *Propontocypris* show lower mean relative abundances prior to the MBE (Table 1). *Henryhowella* shows a mean relative pre-MBE abundance of around 7.3% compared to a mean relative post-MBE abundance of nearly 32% (Table 1). *Polycope* was mainly absent prior to the MBE, except for a few sudden spikes in abundance during MIS 15, in which it is a very abundant taxon within the ostracod assemblage, and often even the sole dominant taxon (Figure 6). After the MBE, *Polycope* occurred commonly from MIS 5 onwards (Figure 6). *Krithe* dominates assemblages before the MBE and up until around 260ka (Figure 6). From MIS 7 onwards, they remain a very abundant component of the ostracod assemblage, but with lower relative abundance values. Although *Krithe* in general appears very abundant within the assemblages before the MBE, there are species-specific differences. Whereas *Krithe hunti*

shows a mean relative abundance of above 60% before the MBE, its post-MBE mean relative abundance reaches only roughly 16% (Table 1). Figure 7 illustrates this drop, which occurred at around 260ka onwards. Before 260ka, *Krithe hunti* appears frequently with a relative abundance of up to 100% of the total species assemblages. After 260ka however, it decreases to less than 40% of relative abundance, occurring primarily during glacials (Figure 7). *Krithe minima*, on the other hand, is extremely rare before the MBE, with a mean relative abundance of around 0.8% as opposed to nearly 19% after the MBE (Table 1). In the present-day Nordic seas, *K. minima* is a fairly common inhabitant (Figure 7). Total abundance is lower prior to the MBE with an average raw count per sample of 67, as opposed to 143 after the MBE (Table 1). The above-mentioned faunal compositional changes are well reflected in the nMDS plot (Figure 8), showing a clear separation of pre- and post-MBE assemblages (with some overlaps though) (PERMANOVA: $F = 44.61$,

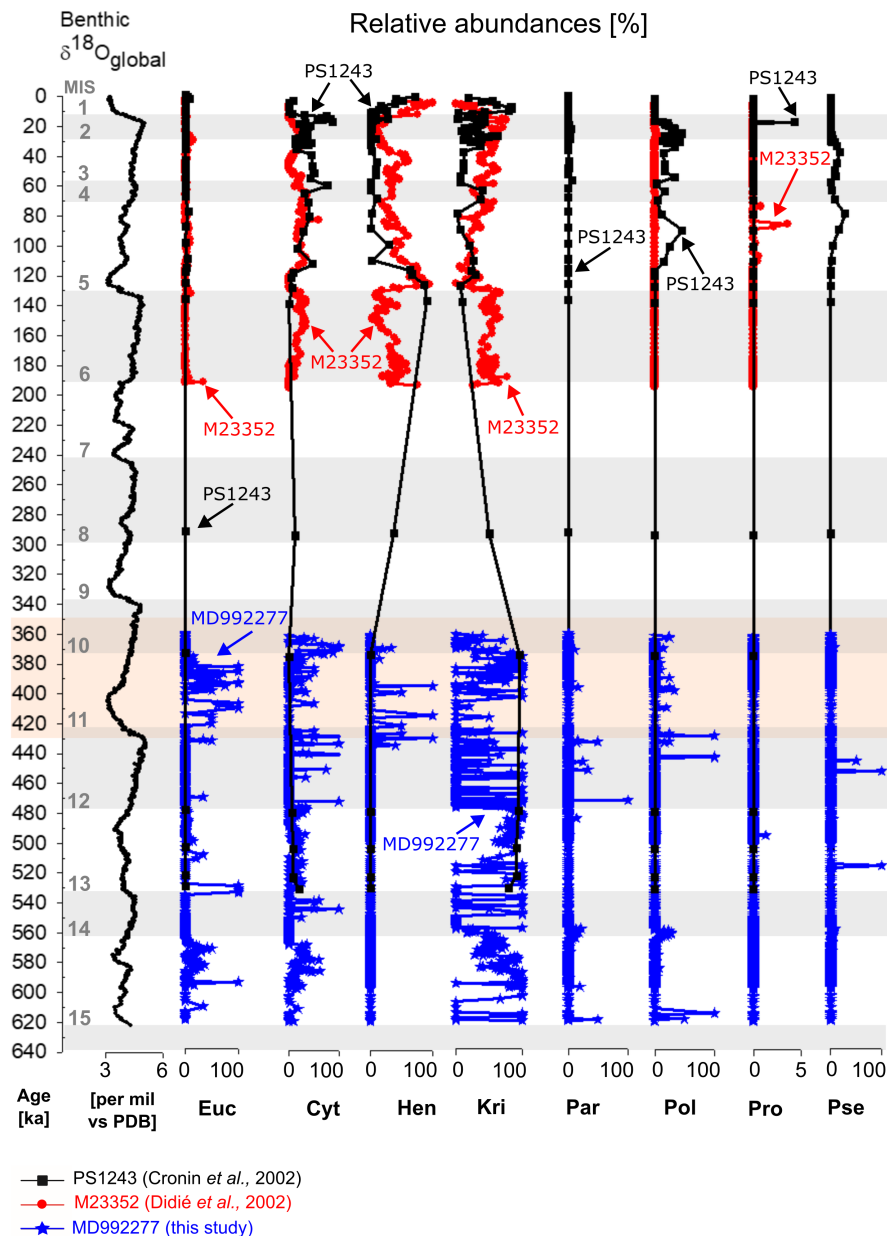
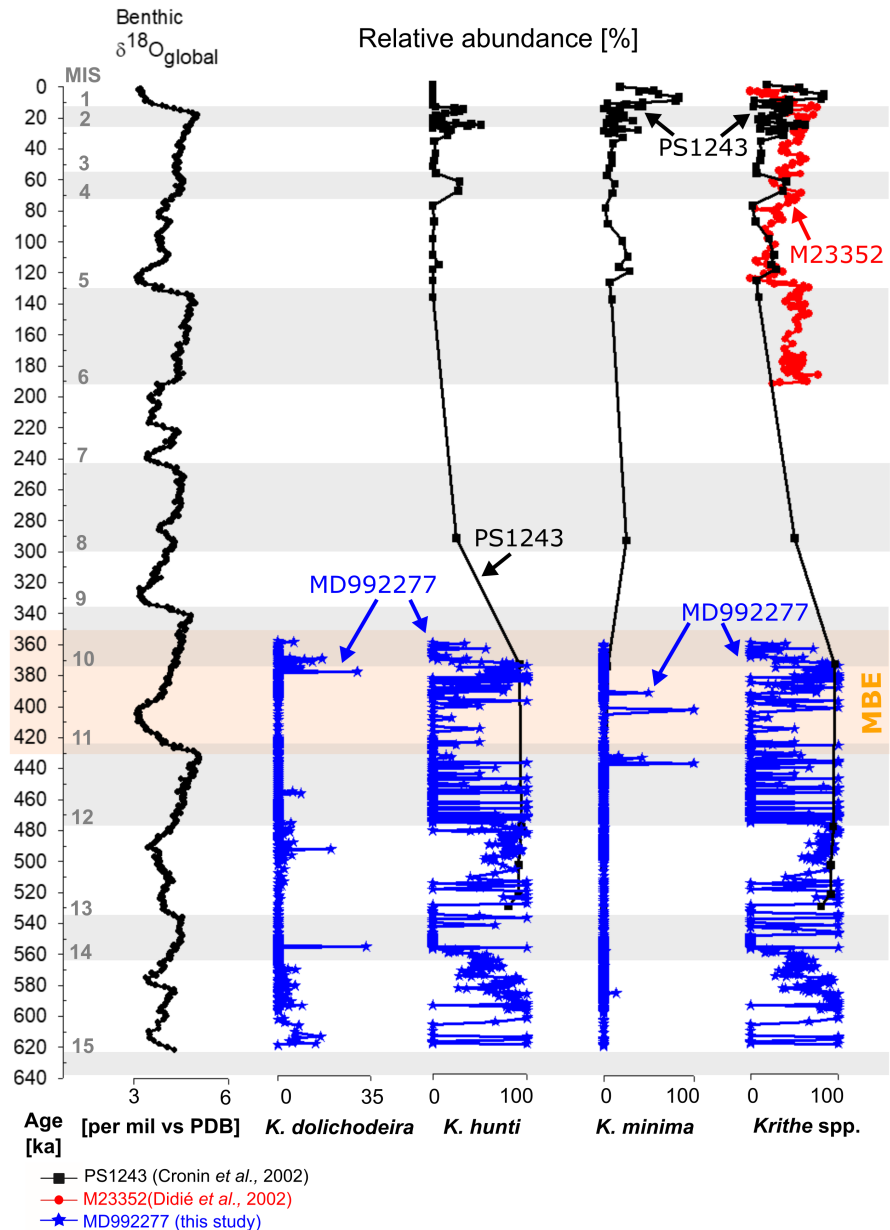


FIGURE 6 Time series changes in abundance of major ostracod genera from ~630ka to present day. Taxa are annotated by their abbreviations: *Cytheropteron* (Cyt), *Eucythere* (Euc), *Henryhowella* (Hen), *Krithe* (Kri), *Paracytherois* (Par), *Polycope* (Pol), *Propontocypris* (Pro) and *Pseudocythere* (Pse). Black squares denote ostracod data obtained from core PS1243 (Cronin et al., 2002); red dots denote ostracod data obtained from core M23352 (Didié et al., 2002); blue stars denote ostracod data obtained from core MD992277 (this study). Abundance given as raw specimen counts (including all samples, no specimen cut-off applied). MIS: Marine Isotope Stage; grey highlighted areas indicate glacial periods (even MIS); white highlighted areas indicate interglacial periods (odd MIS); Mid-Brunhes Event indicated by bisque colour bar from 350 to 430ka (according to Yin and Berger [2010] and Cronin et al. [2017]). Global climate curve (i.e. deep-sea oxygen isotope record) from Lisiecki and Raymo (2005).

FIGURE 7 Comparison of major species of *Krithe* to global benthic $\delta^{18}\text{O}$ changes from ~630ka to present day. Black squares denote ostracod data obtained from core PS1243 (Cronin et al., 2002); red dots denote ostracod data obtained from core M23352 (only *Krithe* genus level data available) (Didié et al., 2002); blue stars denote ostracod data obtained from core MD992277 (this study). *Krithe* spp. here shows the complete *Krithe* record from each core, that is specimens of *K. hunti* and *K. minima* (PS1243), and *K. hunti*, *K. minima*, *K. dolichodeira*, and specimens with unclear species identification (MD992277). M23352 has a *Krithe* record with uncertain species information, hence is excluded from the individual species graphs. Abundance given as relative abundance within the assemblage [%]. MIS: Marine Isotope Stage; grey highlighted areas indicate glacial periods (even MIS); white highlighted areas indicate interglacial periods (odd MIS); Mid-Brunhes Event indicated by bisque colour bar from 350 to 430 ka (according to Yin and Berger [2010] and Cronin et al. [2017]).



$p < 0.001$). *Henryhowella* has the highest value on the negative end of nMDS2, characterizing post-MBE samples (Figure 8). Several uncommon genera that exclusively occur in pre-MBE samples, such as *Rosaliella* and *Thaerocythere*, have the highest positive values of nMDS2. *Pseudocythere* and *Polycope* have the highest values on the positive end of nMDS1, characterizing some samples of the two, more closely located sites, PS1243 and MD992277.

3.3 | Diversity dependence on abundance, and diversity and abundance dependencies on sedimentation rate

Abundance versus diversity cross plots revealed that, compared to raw diversity measures, estimated Hill numbers substantially reduce the abundance dependency of diversity (see R^2 values on Figure S2,

given as Appendix 6 in Online Supplement S1). We also contrasted sedimentation rate with diversity to illuminate potential temporal grain bias affecting the time averaging. The respective plot revealed that there is no significant relationship between diversity and sedimentation rate (see p-values on bottom panel of Figure S2, given as Appendix 6 in Online Supplement S1).

4 | DISCUSSION

4.1 | Has the deep Norwegian Sea diversity been suppressed by quaternary glaciation?

Our results show that deep Norwegian Sea diversity was not suppressed by Quaternary glaciation, with post-MBE glacial diversity tending to be notably higher than that of interglacial periods

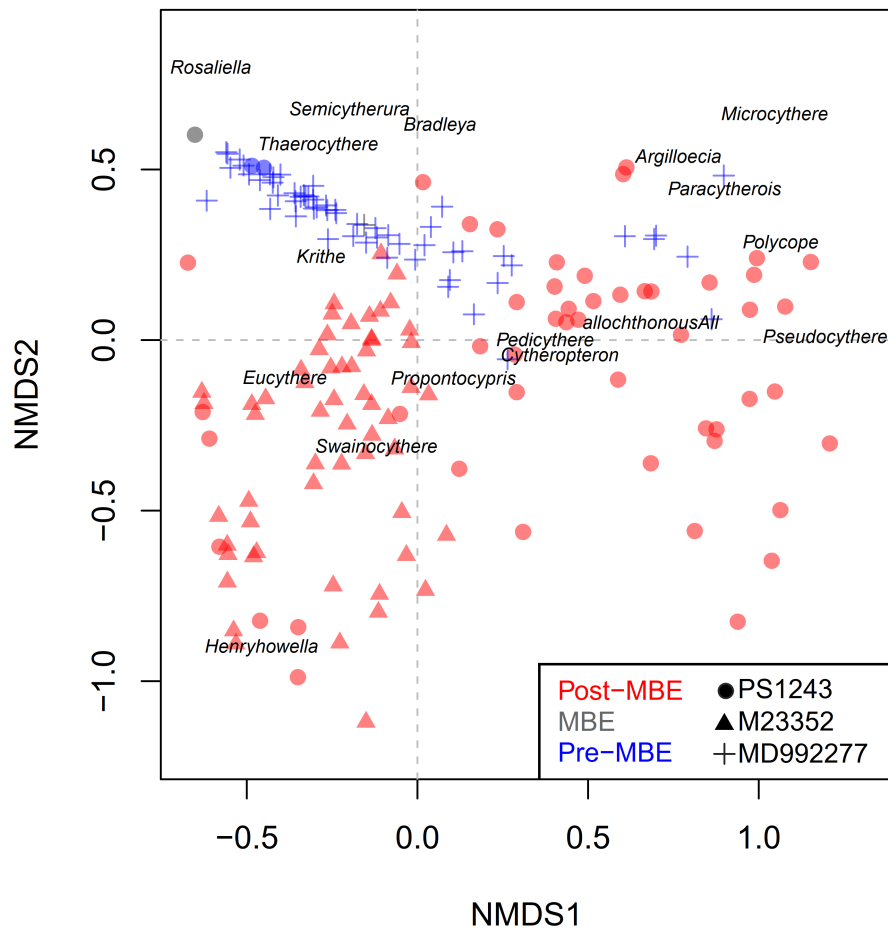


FIGURE 8 Non-metric multidimensional scaling (nMDS) plot of the faunal assemblages. PS1243 samples are indicated by dots, M23352 samples by plus-signs, and MD992277 samples by plus-signs. Pre-MBE samples (older than 430 ka) are indicated by blue symbols; MBE samples (between 430 and 350 ka) are indicated by grey symbols, and post-MBE samples (younger than 350 ka) are indicated by red symbols. Uneven cut-off thresholds were applied to have a similar number of samples from each core: at least 20 specimens for PS1243 (number of samples $N=52$), 150 for M23352 (number of samples $N=58$), 100 for MD992277 (number of samples $N=58$). The stress value of ~ 0.1 indicates that the preservation of multivariate distance in the nMDS configuration is within good to acceptable range, quantitatively supporting the observed compositional changes.

(Figures 4 and 5). Especially for MIS 2–4, alpha (particularly in respect to rare species; $q=0$) and gamma diversities are high (Figure 5). Therefore, the fundamental precondition of the glacial disturbance hypothesis is not supported.

The high MIS 2–4 diversities may be caused by the comparably high intermediate water temperature at that time (Cronin et al., 2017). Indeed, MIS 6 was considerably cooler and shows lower diversities according to our data (Figures 4 and 5). On the other hand, diversities during MIS 10 and 14, respectively, are high, despite the lack of high temperature indications (Cronin et al., 2017), which could point to other mechanisms operating diversity changes. Our data show that during MIS 2–4, the diversity of rare species ($q=0$) is high, while during MIS 10 and 14, respectively, the diversity of dominant species ($q=2$) is high (especially for MIS 14, it is higher than during MIS 2–4) (Figure 5). A possible explanation for these notable differences could be species-specific sensitivities to changes in surface production. Low or changing surface production may allow the coexistence of relatively many dominant species, as it is known that high productivity often leads to the dominance by only few opportunistic species (as seen in the case of eutrophication; Yasuhara, Hunt, Breitburg, et al., 2012). Changes in abundance and sedimentation rate should not have significantly distorted the general results of this study. Estimated Hill numbers substantially reduce the abundance dependency of diversity compared to raw diversity measures (i.e. observed Hill numbers), and there is no statistical relationship

between estimated Hill numbers and averaged sedimentation rates that is higher diversities are not caused merely by lower sedimentation rates (i.e. higher time averaging) (Figure S2, given as Appendix 6 in Online Supplement S1).

Our results, based on alpha and gamma diversities, are reasonably comparable to deep-sea biological studies reporting low Norwegian Sea diversity (Culver & Buzas, 2000; Dahl, 1979; Jöst et al., 2019; Lamshead et al., 2000; Rex et al., 1993, 2000; Svavarsson, 1997; Svavarsson et al., 1993; Yasuhara, Hunt, et al., 2009; Yasuhara, Hunt, Cronin, et al., 2012). Indeed, glacial environments in the deep Norwegian Sea are characterized by lower surface productivity that positively affected deep-sea diversity (Didié et al., 2002). Since it is known that diversity and surface productivity (the main food source of deep-sea benthos as particulate organic carbon flux) have a unimodal relationship (Tittensor et al., 2011) and the Norwegian Sea productivity is high (Lutz et al., 2007), it is reasonable that we see a negative relationship between diversity and productivity, as it represents the descending rim of this unimodal relationship with increasing dominance of few opportunistic species. The glacial Norwegian Sea was covered by sea ice, but only seasonally (Pflaumann et al., 2003). This ice cover probably decreased surface productivity, as mentioned above. The seasonal nature of sea ice caused the deposition of ice-rafted debris (IRD), lithic grains of terrestrial origin brought in by drift-ice when the ice melted (Bond et al., 1997, 2001; Heinrich, 1988). But it is known that deep-sea diversity actually increased during periods

of intensive IRD deposition, a phenomenon known as Heinrich events (Heinrich, 1988), probably because (1) surface productivity was lower during these events and/or (2) the soft sediment habitat was disturbed or habitat heterogeneity was increased by the IRD deposition (Yasuhara & Cronin, 2008). Similarly, ostracod abundance also does not show a clear trend of low glacial values (Figure 3). However, benthic foraminiferans reportedly show lower glacial abundance in the deep Norwegian Sea (Struck, 1995). This probably indicates the well-known sensitivity of benthic foraminiferans to food supply (Goody, 2003; Herguera, 2000; Nees et al., 1999; Rasmussen et al., 2003; Yasuhara, Hunt, Cronin, et al., 2012). In addition, recent paleoceanographic studies indicate that, in the subpolar North Atlantic and Arctic, glacial and stadial deep-sea (especially intermediate water) temperature was warmer than during interglacial and interstadial periods (Cronin et al., 2012; Marcott et al., 2011; Rasmussen & Thomsen, 2004; Yasuhara et al., 2019; Yasuhara, Okahashi, et al., 2014). In sum, our result and also results from other paleoecological and paleoceanographic studies, consistently show that the glacial deep Norwegian Sea environment was not particularly harsh for deep-sea benthos and their biodiversity.

Rather, the present-day-style deep Norwegian Sea ecosystem was established by an MBE-induced shift in climate. The direct trigger of the MBE faunal shift and changes in pre-MBE and post-MBE diversity is difficult to explain, and probably complex. There are several possible reasons, first, the exchange between the North Atlantic proper waters and the Nordic Seas: Stronger post-MBE glacials have led to a much lower sea level after the MBE, which might have caused a stronger isolation of the Nordic-Arctic region. This may also explain the pre-MBE presence of Atlantic taxa and their post-MBE disappearance (DeNinno et al., 2015). A second reason could be the generally much warmer intermediate water temperature in the region (except Deglacial-Holocene; see Cronin et al., 2017). As the temperature-diversity relationship is significantly positive in ostracods (at least in lower-temperature geographic ranges; see Jöst et al., 2019), warmer post-MBE intermediate water temperatures could be another reason for higher post-MBE diversity, although the gamma diversity is lower in the post-MBE period (Figure S1, given as Appendix 4 in Online Supplement S1). A third possible reason is changes in sea ice. The pre- and post-MBE sea ice regimes were different, with the pre-MBE Arctic region having experienced ice-free conditions more frequently (Cronin et al., 2017). This might have affected surface productivity and POC flux, resulting in the observed ostracod faunal composition. Overall however, more data are needed to reach a better, more comprehensive conclusion.

4.2 | Did the MBE play a role in establishing the deep Norwegian Sea ecosystem, including faunal composition and biodiversity?

While we did not see a consistent difference between pre- and post-MBE diversities in alpha and gamma diversities (Figure S1, given as Appendix 4 in Online Supplement S1), we found a substantial faunal shift

across the MBE (Figure 6). For example, *Henryhowella*, abundant during and after the MBE, is primarily absent in pre-MBE samples (Figure 6). *Propontocypris* shows a similar trend, being more common in post-MBE samples (Figure 6). In contrast, *Eucythere* and *Paracytherois* are abundant in many pre-MBE samples, but are very rare in post-MBE samples (Figure 6). *Krithe* is dominant almost throughout the record, but comparatively more abundant in pre-MBE samples than in post-MBE ones. Since *Eucythere* is known as an indicator of seasonal surface production (Didié et al., 2002), and *Henryhowella* and *Krithe* are probably sensitive and tolerant to low oxygen conditions, respectively (Yasuhara & Cronin, 2008), we speculate that the MBE faunal shift in the Norwegian Sea is related to a shift in the surface productivity mode, and thus in food supply and the oxygen state in the deep sea, while further details remain elusive. *Krithe dolichodeira*, a species with a modern distribution limited to the North Atlantic proper (i.e. on the south side of Iceland) is absent in post-MBE samples, but abundant in MBE and pre-MBE samples (Figure 7). *Krithe hunti* and *Krithe minima* on the other hand, both extant species in the Norwegian Sea and the Arctic Ocean (Jöst et al., 2022; Yasuhara, Grimm, et al., 2014), show contrasting abundance patterns. While *Krithe hunti* is more abundant in pre-MBE samples, *Krithe minima* tends to be more abundant in post-MBE samples (Figure 7). Generic faunal shifts and faunal differences across the MBE are clearly shown in the nMDS plot (Figure 8). A similar strong faunal shift is also known from the high Arctic (Cronin et al., 2017; DeNinno et al., 2015). *Acetabulastoma* and *Polycope* are abundant after the MBE but very rare before the MBE (Cronin et al., 2017). Several taxa, such as *Echinocythereis*, *Arcacythere*, and several species of *Krithe* (including *Krithe dolichodeira*), are absent in the present-day and post-MBE Arctic, but they were abundant before the MBE (DeNinno et al., 2015). While parts of the faunal shift are different between the Norwegian Sea and Arctic Ocean (e.g. *Polycope* does not show a clear trend in the Norwegian Sea; *Henryhowella* shows opposite pattern between the Norwegian Sea and Arctic Ocean) (Figure 6), this largely consistent faunal shift indicates that the MBE played an important role in the establishment of the present-day polar deep-sea ecosystem by initiation of compositional changes with possible consecutive impacts on biodiversity. Ecological causes of the very low, present-day Norwegian Sea diversity were tested in a previous macroecological study, resulting in the conclusion that the barrier effect caused by the Greenland-Iceland-Faeroe Ridge (i.e. physical and hydrochemical barrier through strong temperature and productivity gradients along the ridge) in combination with the present-day very low water temperature, are responsible for the Nordic Seas' low diversity in, especially meiobenthos with limited dispersal abilities (Jöst et al., 2019). But it is still elusive, why such diversity decline has occurred in the Holocene, but not in the many pre-Holocene interglacials.

4.3 | Limitations of study

4.3.1 | Taxonomic bias

Our study is based on a combined data set of alpha diversities from three coring sites of different locations and depths, obtained

by three types of corers. These heterogeneities in sampling, as well as taxonomic bias based on species identification by several, individual taxonomists, could potentially account for some of the observed differences in diversity and composition, unrelated to ecological causes. However, all three cores generally show a solid data comparability by examining published scanning electron microscope (SEM) images from the cores M23352 and PS1243 (Cronin et al., 2002; Didié et al., 2002; Didié & Bauch, 2002). Generally, faunal compositions of both cores are very similar, especially on genus level. Both show a high presence of *Krithe* and *Cytheropteron* specimens, and other major taxa (*Henryhowella*, *Polycope*, *Eucythere*, *Propontocypris*) are present in both cores (Table S4, given as Appendix 7 in Online Supplement S1). The record of M23352 lists specimens of *Swainocythere*, *Nannocythere* and *Microcythere?*, all of which do not occur in the PS1243 record (Table S4, given as Appendix 7 in Online Supplement S1). This could indicate ecological differences at the two coring locations, although it appears more likely that these differences reflect sample size effect and varying completeness of raw data. Sample effort is likely the cause for the appearance of additional rare taxa in M23352 that are lacking in PS1243, as more samples were picked (143 vs. 61), covering a shorter time frame (190.3 kyrs vs 530.7 kyrs) (Table S1, given as Appendix 1 in Online Supplement S1). Therefore, to further reduce taxonomic bias, while keeping full insight into our interpretative basis and avoiding statistical misinterpretation, for nMDS, we deliberately used genus-level counts only. Genus-level taxonomy was confirmed prior to analyses based on the SEMs provided in the respective publications, hence taxonomic identification on genus level is considered unaffected by taxonomic bias. In respect to census data, for PS1243 and M23352, we do not have any record of ostracod-barren samples, whereas for our own core, MD992277, we do have that record. This discrepancy only plays a role when plotting abundance over time, as the plots lacking barren samples appear smoother (see Figures 6 and 7).

4.3.2 | Discontinuous time record

Given the very limited amount of data immediately following the MBE (basically no data in MIS 9, 8, 7, except for a single PS1243 sample during MIS 8), there is the possibility that some event during this period, other than the MBE, could have had some influence on the observed faunal shift. However, faunal turnovers of microfossil communities recorded by deep-sea sediment long-cores from the Arctic Ocean have shown to be driven by fundamental shifts in sea-ice cover variability, surface primary production, and Arctic Ocean temperature as consequences of MBE-enhanced Arctic Amplification (i.e. amplified warming in Arctic regions relative to the global mean temperature) (Cronin et al., 2017; DeNinno et al., 2015). Therefore, it appears plausible, that our faunal turnover in the Norwegian Sea, which is adjacent to the Arctic Ocean, similarly, was set off during and because of the MBE, and was not caused by a later event for

which we lack data. Further limitations are described in detail in Appendix.

5 | CONCLUSION

Our fossil study enabled the testing of the deep-sea glacial disturbance hypothesis as a cause of the low, present-day Norwegian Sea diversity and the resulting steep latitudinal diversity gradient. We found that Norwegian Sea deep-sea diversity based on ostracod fossils was higher during the last glacial than during the present interglacial. Hence, our findings did not support the deep-sea glacial disturbance hypothesis. Instead, the present-day deep Norwegian Sea ecosystem was likely established by the Mid-Brunhes Event, and the major faunal shifts and, perhaps, extinctions, resulting from this Pleistocene climate transition. In a broader context, we may conclude that the MBE has played an important role in the establishment of the present-day-style polar deep-sea ecosystem and biodiversity in general.

AUTHOR CONTRIBUTIONS

A.B.J. and M.Y. designed the research. A.B.J., H.O. and M.Y. picked and taxonomically identified MD992277 specimens. A.B.J., H.H.M.H., Y.H. and C.-L.W. performed the data handling and statistical analyses and generated the figures. H.A.B. provided MD992277 sediment samples. T.M.C. provided ostracod assemblage raw data of cores PS1243 and M23352. H.B. provided the raw data for the new age model of core PS1243. B.T. provided critical feedback. A.B.J. and M.Y. wrote the paper in collaboration with all authors.

ACKNOWLEDGMENTS

We thank Laura Wong, Cecily Law and Maria Lo for assistance in laboratory-related matters, Jan P. Helmke from the GEOMAR Helmholtz Center for Ocean Research Kiel (Germany) for providing chronological raw data of core MD992277, and Prof. Dr. Alan Lord from the Senckenberg Research Institute in Frankfurt am Main (Germany) for hosting A.B.J. as guest researcher in the Micropalaeontology department to work on sections of core MD992277, and Laura Gemery and Marci M. Robinson for their pre-submission comments in fulfilment with U.S. Geological Survey regulations. We also highly appreciate the quality and depth of comments by the handling editor, Dr. Adam Tomašových and the two anonymous reviewers, which contributed to sincerely improving this manuscript. The work described in this study was partially supported by grants from the Research Grants Council of the Hong Kong Special Administrative Region, China (project codes: RFS2223-7S02 to M.Y., HKU 17311316 to M.Y., HKU 17301818 to B.T.), the Seed Funding Program for Basic Research of the University of Hong Kong (reference codes: 2202100581, 202,011,159,122, 201,210,159,043, 201,511,159,075, 201,411,159,017 to M.Y.), the Faculty of Science RAE Improvement Fund of the University of Hong Kong (to M.Y.), and the Ecology and Biodiversity Division Fund (reference code: 5594129 to A.B.J.). The writing and figure-plotting

process was financially supported by the Brain Pool Program through NRF funded by the Ministry of Science and ICT (reference code: 2019H1D3A1A01070922 to A.B.J.). H.H.M.H. was supported by Peter Buck Postdoc Fellowship, Smithsonian Institution. T.M.C was funded by the U.S. Geological Survey Climate Research and Development Program. Any use of trade, firm, or product names is for descriptive purposes only and does not imply endorsement by the U.S. Government.

CONFLICT OF INTEREST STATEMENT

The authors declare that there is no conflict of interest regarding the publication of this article.

DATA AVAILABILITY STATEMENT

The data that supports the findings of this study are available in the supplementary material of this article.

ORCID

Anna B. Jöst  <https://orcid.org/0000-0002-1289-3630>

Chih-Lin Wei  <https://orcid.org/0000-0001-9430-0060>

Moriaki Yasuhara  <https://orcid.org/0000-0003-0990-1764>

REFERENCES

- Anderson, M. J., & Walsh, D. C. (2013). PERMANOVA, ANOSIM, and the mantel test in the face of heterogeneous dispersions: What null hypothesis are you testing? *Ecological Monographs*, *83*, 557–574.
- Augstein, E., Hempel, G., Schwarz, J. & Thiede, J. (1984) Die Expedition Arktis II des FS "Polarstern" 1984 mit den Beiträgen des FS "Valdivia" und des Forschungsflugzeuges "Falcon 20" zum Marginal Ice Zone Experiment 1984 (MIZEX).
- Bauch, H. A. (1997). Paleoceanography of the North Atlantic Ocean (68°–76°N) during the past 450 ky deduced from planktic foraminiferal assemblages and stable isotopes. In H. C. Hass & M. A. Kaminski (Eds.), *Contributions to the micropaleontology and paleoceanography of the Northern North Atlantic* (pp. 83–100). Grzybowski Foundation Special Publication, no. 5.
- Bauch, H. A., Erlenkeuser, H., Helmke, J. P., & Struck, U. (2000). A paleoclimatic evaluation of marine oxygen isotope stage 11 in the high-northern Atlantic (Nordic seas). *Global and Planetary Change*, *24*, 27–39.
- Bauch, H. A., & Helmke, J. P. (1999). Glacial-interglacial records of the reflectance of sediments from the Norwegian-Greenland-Iceland Sea (Nordic seas). *International Journal of Earth Sciences*, *88*, 325–336.
- Bauch, H. A., & Kandiano, E. S. (2007). Evidence for early warming and cooling in North Atlantic surface waters during the last interglacial. *Paleoceanography*, *22*, PA1201.
- Bauch, H. A., Struck, U., & Thiede, J. (2001). Planktic and benthic Foraminifera as indicators of past ocean changes in surface and deep waters of the Nordic seas. In P. Schäfer, W. Ritzrau, M. Schlüter, & J. Thiede (Eds.), *The Northern North Atlantic* (pp. 411–421). Springer Verlag Berlin Heidelberg.
- Bodil, B. A., Ambrose, W. G., Bergmann, M., Clough, L. M., Gebruk, A. V., Hasemann, C., Iken, K., Klages, M., MacDonald, I. R., Renaud, P. E., Schewe, I., Soltwedel, T., & Włodarska-Kowalczyk, M. (2011). Diversity of the arctic deep-sea benthos. *Marine Biodiversity*, *41*, 87–107.
- Bond, G., Kromer, B., Beer, J., Muscheler, R., Evans, M. N., Showers, W., Hoffmann, S., Lotti-Bond, R., Hajdas, I., & Bonani, G. (2001). Persistent solar influence on North Atlantic climate during the Holocene. *Science*, *294*, 2130–2136.
- Bond, G., Showers, W., Cheseby, M., Lotti, R., Almasi, P., Priore, P., Cullen, H., Hajdas, I., & Bonani, G. (1997). A pervasive millennial-scale cycle in North Atlantic Holocene and glacial climates. *Science*, *278*, 1257–1266.
- Borcard, D., Gillet, F., & Legendre, P. (2011). *Numerical ecology with R*. Springer Verlag. Read online: <http://library.lol/main/9BA82597FD A7D4D4A2F1C1CA128C2480>
- Chao, A., Gotelli, N. J., Hsieh, T. C., Sander, E. L., Ma, K. H., Colwell, R. K., & Ellison, A. M. (2014). Rarefaction and extrapolation with Hill numbers: A framework for sampling and estimation in species diversity studies. *Ecological monographs*, *84*, 45–67.
- Chao, A., Kubota, Y., Zelený, D., Chiu, C.-H., Li, C.-F., Kusumoto, B., Yasuhara, M., Thorn, S., Wei, C.-L., Costello, M. J., & Colwell, R. K. (2020). Quantifying sample completeness and comparing diversities among assemblages. *Ecological Research*, *35*, 292–314.
- Chiu, W. R., Yasuhara, M., Cronin, T. M., Hunt, G., Gemery, L., & Wei, C. (2020). Marine latitudinal diversity gradients, niche conservatism and out of the tropics and Arctic: Climatic sensitivity of small organisms. *Journal of Biogeography*, *47*, 817–828.
- Coles, G. P., Whatley, R. C., & Mognilevsky, A. (1994). The ostracode genus *Krithe* from the Tertiary and Quaternary of the North Atlantic. *Palaeontology*, *37*, 71–120.
- Corliss, B. H., Brown, C. W., Sun, X., & Showers, W. J. (2009). Deep-sea benthic diversity linked to seasonality of pelagic productivity. *Deep Sea Research Part I: Oceanographic Research Papers*, *56*, 835–841.
- Cronin, T. M. (1989). Paleozoogeography of postglacial Ostracoda from Northeastern North Atlantic. In N. R. Gadd (Ed.), *The late quaternary development of the Champlain Sea basin special paper* (pp. 125–144). Geological Association of Canada.
- Cronin, T. M., DeNinno, L. H., Polyak, L., Caverly, E. K., Poore, R. Z., Brenner, A., Rodriguez-Lazaro, J., & Marzen, R. E. (2014). Quaternary ostracode and foraminiferal biostratigraphy and paleoceanography in the western Arctic Ocean. *Marine Micropaleontology*, *111*, 118–133.
- Cronin, T. M., Dwyer, G. S., Caverly, E. K., Farmer, J., DeNinno, L. H., Rodriguez-Lazaro, J., & Gemery, L. (2017). Enhanced Arctic amplification began at the mid-Brunhes event ~400,000 years ago. *Scientific Reports*, *7*, 14475.
- Cronin, T. M., Dwyer, G. S., Farmer, J., Bauch, H. A., Spielhagen, R. F., Jakobsson, M., Nilsson, J., Briggs, W. M., & Stepanova, A. (2012). Deep Arctic Ocean warming during the last glacial cycle. *Nature Geoscience*, *5*, 631–634.
- Cronin, T. M., Boomer, I., Dwyer, G. S., & Rodríguez-Lázaro, J. (2002). Ostracoda and paleoceanography. In J. A. Holmes & A. R. Chivas (Eds.), *The Ostracoda: Applications in quaternary research* (Vol. 131, pp. 99–119). Geophysical Monograph.
- Cronin, T. M., Gemery, L., Briggs, W. M., Jakobsson, M., Polyak, L., & Brouwers, E. M. (2010). Quaternary sea-ice history in the Arctic Ocean based on a new ostracode sea-ice proxy. *Quaternary Science Reviews*, *29*, 3415–3429.
- Culver, S. J., & Buzas, M. A. (2000). Global latitudinal species diversity gradient in deep-sea benthic Foraminifera. *Deep Sea Research Part I: Oceanographic Research Papers*, *47*, 259–275.
- Dahl, E. (1979). Amphipoda Gammaridea from the deep Norwegian Sea. A Preliminary Report. *Sarsia*, *64*, 57–59.
- DeNinno, L. H., Cronin, T. M., Rodriguez-Lazaro, J., & Brenner, A. (2015). An early to mid-Pleistocene deep Arctic Ocean ostracode fauna with North Atlantic affinities. *Palaeogeography, Palaeoclimatology, Palaeoecology*, *419*, 90–99.
- Didié, C., & Bauch, H. A. (2002). Implications of upper Quaternary stable isotope records of marine ostracodes and benthic foraminifers for paleoecological and paleoceanographical investigations. In J.

- A. Holmes & A. R. Chivas (Eds.), *Geophysical monograph series* (pp. 279–299). American Geophysical Union.
- Didié, C., Bauch, H. A., & Helmke, J. P. (2002). Late Quaternary deep-sea ostracodes in the polar and subpolar North Atlantic: Paleocological and paleoenvironmental implications. *Palaeogeography, Palaeoclimatology, Palaeoecology*, *184*, 195–212.
- Elliot, M., Labeyrie, L., Bond, G., Cortijo, E., Turon, J.-L., Tisnerat, N., & Duplessy, J.-C. (1998). Millennial-scale iceberg discharges in the Irminger Basin during the last glacial period: Relationship with the Heinrich events and environmental settings. *Paleoceanography*, *13*, 433–446.
- Gemery, L., Cronin, T. M., Briggs, W. M., Jr., Brouwers, E. M., Schornikov, E. I., Stepanova, A. Y., Wood, A. M., & Yasuhara, M. (2015). An Arctic and Subarctic ostracode database: Biogeographic and paleoceanographic applications. *Hydrobiologia*, *786*, 59–95.
- Gooday, A. J. (2003). Benthic Foraminifera (Protista) as tools in deep-water palaeoceanography: Environmental influences on faunal characteristics. In A. J. Southward (Ed.), *Advances in marine biology* (pp. 3–91). Elsevier.
- Hayward, B. W., Kawagata, S., Grenfell, H. R., Sabaa, A. T., & O'Neill, T. (2007). Last global extinction in the deep sea during the mid-Pleistocene climate transition. *Paleoceanography*, *22*, PA3103.
- Hayward, B. W., Kawagata, S., Sabaa, A., Grenfell, H., Kerckhoven, L. V., Johnson, K., & Thomas, E. (2012). The last global extinction (Mid-Pleistocene) of deep-sea benthic Foraminifera (Chrysalogoniidae, Ellipsoidinidae, Glandulonodosariidae, Plectofrondiculariidae, Pleurostomellidae, Stilostomellidae), their Late Cretaceous–Cenozoic history and taxonomy. *Cushman Foundation for Foraminiferal Research*, *43*, 409.
- Heinrich, H. (1988). Origin and consequences of cyclic ice rafting in the Northeast Atlantic Ocean during the past 130,000 years. *Quaternary Research*, *29*, 142–152.
- Helmke, J. P., & Bauch, H. A. (2003). Comparison of glacial and interglacial conditions between the polar and subpolar North Atlantic region over the last five climatic cycles. *Paleoceanography*, *18*, 2002PA000794.
- Helmke, J. P., Bauch, H. A., & Erlenkeuser, H. (2003). Development of glacial and interglacial conditions in the Nordic seas between 1.5 and 0.35 Ma. *Quaternary Science Reviews*, *22*, 1717–1728.
- Helmke, J. P., Bauch, H. A., & Mazaud, A. (2003). Evidence for a mid-Pleistocene shift of ice-drift pattern in the Nordic seas. *Journal of Quaternary Science*, *18*(2), 183–191. <https://doi.org/10.1002/jqs.735>
- Herguera, J. C. (2000). Last glacial paleoproductivity patterns in the eastern equatorial Pacific: Benthic Foraminifera records. *Marine Micropaleontology*, *40*, 259–275.
- Hirschleber, H., Theilen, F., Balzer, W., von Bodungen, B., & Thiede, J. (1988). *Forschungsschiff Meteor, Reise 7, vom 1. Juni bis 28. September 1988. Report SFB 313*, 10 (pp. 1–257). Kiel University.
- Hsieh, T. C., Ma, K. H., & Chao, A. (2020). iNEXT: iNterpolation and EXTrapolation for species diversity. R package version 2.0.20. <http://chao.stat.nthu.edu.tw/wordpress/software-download/>. https://www.imsbio.co.jp/RGM/R_rdfile?f=iNEXT/man/iNEXT-package.Rd&d=R_CC
- Huang, H.-H. M., Yasuhara, M., Iwatani, H., Yamaguchi, T., Yamada, K., & Mamo, B. (2019). Deep-sea ostracod faunal dynamics in a marginal sea: Biotic response to oxygen variability and mid-Pleistocene global changes. *Paleobiology*, *45*, 85–97.
- Huang, H. M., Yasuhara, M., Iwatani, H., Alvarez Zarikian, C. A., Bassetti, M., & Sagawa, T. (2018). Benthic biotic response to climate changes over the last 700,000 years in a deep marginal sea: Impacts of deoxygenation and the Mid-Brunhes Event. *Paleoceanography and Paleoclimatology*, *33*, 766–777.
- Jellinek, T., Swanson, K., & Mazzini, I. (2006). Is the cosmopolitan model still valid for deep-sea podocopid ostracods? With the discussion of two new species of the genus *Pseudobosquetina* Guernet & Moulade, 1994 and *Cytheropteron testudo* (Ostracoda) as case study. *Senckenbergiana Maritima*, *36*, 29–50.
- Jöst, A. B., Okahashi, H., Ostmann, A., Arbizu, P. M., Svavarsson, J., Brix, S., & Yasuhara, M. (2022). Recent deep-sea ostracods of the sub-polar North Atlantic Ocean. *Micropaleontology*, *68*, 291–343.
- Jöst, A. B., Yasuhara, M., Wei, C., Okahashi, H., Ostmann, A., Martínez Arbizu, P., Mamo, B., Svavarsson, J., & Brix, S. (2019). North Atlantic Gateway: Test bed of deep-sea macroecological patterns. *Journal of Biogeography*, *46*, 2056–2066.
- Kandiano, E. S. (2003). Dynamics of the ocean surface in the polar and subpolar North Atlantic over the last 500 000 years. *Berichte zur Polar- und Meeresforschung (Reports on Polar and Marine Research)*, *456*, 92.
- Kandiano, E. S., van der Meer, M. T. J., Bauch, H. A., Helmke, J., Damsté, J. S. S., & Schouten, S. (2016). A cold and fresh ocean surface in the Nordic seas during MIS 11: Significance for the future ocean: Cold and fresh Nordicseas during MIS 11. *Geophysical Research Letters*, *43*, 10929–10937.
- Labeyrie, L., Cortijo, E., Jansen, E., & Balut, Y. (1999). *Les rapports de campagne à la mer à bord du Marion-Dufresne: Campagne Interpole MD99-114/ IMAGES V–Atlantique Nord et mers Actiques du 11/06/99 au 06/09/99*. Institut Polaire Français, Paul-Emile Victor–IPEV.
- Lamshead, P. J. D., Tietjen, J., Ferrero, T., & Jensen, P. (2000). Latitudinal diversity gradients in the deep sea with special reference to North Atlantic nematodes. *Marine Ecology Progress Series*, *194*, 159–167.
- Legendre, P., & Legendre, L. (2012). Chapter 9—Ordination in reduced space. In P. Legendre & L. Legendre (Eds.), *Developments in environmental modelling* (pp. 425–520). Elsevier.
- Leray, M., & Knowlton, N. (2015). DNA barcoding and metabarcoding of standardized samples reveal patterns of marine benthic diversity. *Proceedings of the National Academy of Sciences*, *112*, 2076–2081.
- Lisiecki, L. E., & Raymo, M. E. (2005). A Pliocene–Pleistocene stack of 57 globally distributed benthic $\delta^{18}\text{O}$ records. *Paleoceanography*, *20*, PA1003.
- Lutz, M. J., Caldeira, K., Dunbar, R. B., & Behrenfeld, M. J. (2007). Seasonal rhythms of net primary production and particulate organic carbon flux to depth describe the efficiency of biological pump in the global ocean. *Journal of Geophysical Research*, *112*, C10011.
- Marcott, S. A., Clark, P. U., Padman, L., Klinkhammer, G. P., Springer, S. R., Liu, Z., Otto-Bliesner, B. L., Carlson, A. E., Ungerer, A., Padman, J., He, F., Cheng, J., & Schmittner, A. (2011). Ice-shelf collapse from subsurface warming as a trigger for Heinrich events. *Proceedings of the National Academy of Sciences*, *108*, 13415–13419.
- Nees, S., Armand, L., De Secker, P., Labracherie, M., & Passlow, V. (1999). A diatom and benthic foraminiferal record from the South Tasman Rise (southeastern Indian Ocean): Implications for paleoceanographic changes for the last 200,000 years. *Marine Micropaleontology*, *38*, 69–89.
- Oksanen, J., Guillaume Blanchet, F., Friendly, M., Kindt, R., Legendre, P., McGinn, D., Minchin, P. R., O'Hara, R. B., Simpson, G. L., Solymos, P., Stevens, M. H. H., Szocs, E., & Wagner, H. (2018). *Vegan: Community ecology package* (R package version 2.5-2).
- Pflaumann, U., Sarnthein, M., Chapman, M., d'Abreu, L., Funnell, B., Huels, M., Kiefer, T., Maslin, M., Schulz, H., Swallow, J., van Kreveland, S., Vautravers, M., Vogelsang, E., & Weinelt, M. (2003). Glacial North Atlantic: Sea-surface conditions reconstructed by GLAMAP 2000: Atlantic sea surface conditions. *Paleoceanography*, *18*, C10011.
- Polyak, L., Best, K. M., Crawford, K. A., Council, E.A., & St-Onge, G. (2013). Quaternary history of sea ice in the western Arctic Ocean based on Foraminifera. *Quaternary Science Reviews*, *79*, 145–156.
- Ramirez-Llodra, E., Brandt, A., Danovaro, R., De Mol, B., Escobar, E., German, C. R., Levin, L. A., Arbizu, P. M., Menot, L., Buhl-Mortensen, P., Narayanaswamy, B. E., Smith, C. R., Tittensor, D. P., Tyler, P. A., Vanreusel, A., & Vecchione, M. (2010). Deep, diverse

- and definitely different: Unique attributes of the world's largest ecosystem. *Biosciences*, 7, 2851–2899.
- Rasmussen, T. L., & Thomsen, E. (2004). The role of the North Atlantic Drift in the millennial timescale glacial climate fluctuations. *Palaeogeography, Palaeoclimatology, Palaeoecology*, 210, 101–116.
- Rasmussen, T. L., Thomsen, E., Troelstra, S. R., Kuijpers, A., & Prins, M. A. (2003). Millennial-scale glacial variability versus Holocene stability: Changes in planktic and benthic Foraminifera faunas and ocean circulation in the North Atlantic during the last 60 000 years. *Marine Micropaleontology*, 47, 143–176.
- Rex, M. A., Crame, J. A., Stuart, C. T., & Clarke, A. (2005). Large-scale biogeographic patterns in marine molluscs: A confluence of history and productivity? *Ecology*, 86, 2288–2297.
- Rex, M. A., & Etter, R. J. (2010). *Deep-sea biodiversity—Pattern and scale*. Harvard University Press.
- Rex, M. A., Etter, R. J., & Stuart, C. T. (1997). Large-scale patterns of species diversity in the deep-sea benthos. In R. F. G. Ormond, J. D. Gage, & M. V. Angel (Eds.), *Marine biodiversity (patterns and processes)* (pp. 94–121). Cambridge University Press.
- Rex, M. A., Stuart, C. T., & Coyne, G. (2000). Latitudinal gradients of species richness in the deep-sea benthos of the North Atlantic. *Proceedings of the National Academy of Sciences*, 97, 4082–4085.
- Rex, M. A., Stuart, C. T., Hessler, R. R., Allen, J. A., Sanders, H. L., & Wilson, G. D. F. (1993). Global-scale latitudinal patterns of species diversity in the deep-sea benthos. *Nature*, 365, 636–639.
- Schellenberg, S. A. (2007). Marine ostracods. In *Encyclopedia of quaternary science paleolimnology* (pp. 2046–2062). Elsevier.
- Stepanova, A. Y., Taldenkova, E., & Bauch, H. A. (2004). Ostracod species of the genus *Cytheropteron* from late Pleistocene, Holocene and recent sediments of the Laptev Sea (Arctic Siberia). *Revista Española de Micropaleontología*, 36, 83–108.
- Struck, U. (1995). Stepwise postglacial migration of benthic Foraminifera into the abyssal northeastern Norwegian Sea. *Marine Micropaleontology*, 26, 207–213.
- Stuart, C. T., & Rex, M. A. (2009). Bathymetric patterns of deep-sea gastropod species diversity in 10 basins of the Atlantic Ocean and Norwegian Sea. *Marine Ecology*, 30, 164–180.
- Svavarsson, J. (1997). Diversity of isopods (Crustacea): New data from the Arctic and Atlantic Oceans. *Biodiversity and Conservation*, 6, 1571–1579.
- Svavarsson, J., Stromberg, J.-O., & Brattegard, T. (1993). The deep-sea asellote (Isopoda, Crustacea) fauna of the Northern seas: Species composition, distributional patterns and origin. *Journal of Biogeography*, 20, 537–555.
- Sylvester-Bradley, P. C. (1973). *The New Palaeontology*. Stereo-Atlas of Ostracod Shells.
- Tittensor, D. P., Rex, M. A., Stuart, C. T., McClain, C. R., & Smith, C. R. (2011). Species-energy relationships in deep-sea molluscs. *Biology Letters*, 7, 718–722.
- Whatley, R. C., & Coles, G. P. (1987). The Late Miocene to Quaternary Ostracoda of leg 94, deep sea drilling project. *Revista Española de Micropaleontología*, 19, 33–70.
- Whatley, R. C., Eynon, M. P., & Moguilevsky, A. (1996). Recent Ostracoda of the Scoresby Sund Fjord System, East Greenland. *Revista Española de Micropaleontología*, 28, 5–23.
- Whatley, R. C., Eynon, M. P., & Moguilevsky, A. (1998). The depth distribution of Ostracoda from the Greenland Sea. *Journal of Micropaleontology*, 17, 15–32.
- Wood, A. M. (2005). Revision of the ostracod genus *Celtia* Neale, 1973 and other so-called “tricostate” Trachyleberidinae from the Neogene to recent Europe. *Bollettino della Società Paleontologica Italiana*, 44, 55–80.
- Yasuhara, M. (2018). Marine biodiversity in space and time: What tiny fossils tell. *Mètode Revista de difusió de la investigació*, 98, 61–65.
- Yasuhara, M., & Cronin, T. M. (2008). Climatic influences on deep-sea ostracode (Crustacea) diversity for the last three million years. *Ecology*, 89, S53–S65.
- Yasuhara, M., DeMenocal, P. B., Dwyer, G. S., Cronin, T. M., Okahashi, H., & Huang, H.-H. M. (2019). North Atlantic intermediate water variability over the past 20,000 years. *Geology*, 47, 659–663.
- Yasuhara, M., & Deutsch, C. A. (2022). Paleobiology provides glimpse of future ocean. *Science*, 375, 25–26.
- Yasuhara, M., Grimm, M., Nunes Brandão, S., Jöst, A. B., Okahashi, H., Iwatani, H., Ostmann, A., & Martínez Arbizu, P. (2014). Deep-sea benthic ostracodes from multiple core and epibenthic sledge samples in Icelandic waters. *Polish Polar Research*, 35, 341–360.
- Yasuhara, M., Huang, H.-H., Hull, P., Rillo, M., Condamine, F., Tittensor, D., Kučera, M., Costello, M., Finnegan, S., O'Dea, A., Hong, Y., Bonebrake, T., McKenzie, R., Doi, H., Wei, C.-L., Kubota, Y., & Saupe, E. (2020). Time machine biology: Cross-timescale integration of ecology, evolution, and oceanography. *Oceanography*, 33, 17–28.
- Yasuhara, M., Hunt, G., Breitburg, D., Tsujimoto, A., & Katsuki, K. (2012). Human-induced marine ecological degradation: micropaleontological perspectives. *Ecology and Evolution*, 2, 3242–3268.
- Yasuhara, M., Hunt, G., Cronin, T. M., Hokansishi, N., Kawahata, H., Tsujimoto, A., & Ishitake, M. (2012). Climatic forcing of Quaternary deep-sea benthic communities in the North Pacific Ocean. *Paleobiology*, 38, 162–179.
- Yasuhara, M., Hunt, G., Cronin, T. M., & Okahashi, H. (2009). Temporal latitudinal-gradient dynamics and tropical instability of deep-sea species diversity. *Proceedings of the National Academy of Sciences*, 106, 21717–21720.
- Yasuhara, M., Hunt, G., Dowsett, H. J., Robinson, M. M., & Stoll, D. K. (2012). Latitudinal species diversity gradient of marine zooplankton for the last three million years. *Ecology Letters*, 15, 1–6.
- Yasuhara, M., Hunt, G., & Jordan, R. W. (2022). Macroecology, macroevolution, and paleoecology of Ostracoda. *Marine Micropaleontology*, 174, 102–132.
- Yasuhara, M., Hunt, G., Okahashi, H., & Nunes Brandão, S. (2013). The “*Oxycythereis*” problem: Taxonomy and paleobiogeography of deep-sea ostracod genera *Penyella* and *Rugocythereis*. *Palaeontology*, 56, 1045–1080.
- Yasuhara, M., & Okahashi, H. (2014). Quaternary deep-sea ostracode taxonomy of ocean drilling program site 980, Eastern North Atlantic. *Journal of Paleontology*, 88, 770–785.
- Yasuhara, M., & Okahashi, H. (2015). Late Quaternary deep-sea ostracod taxonomy of the eastern North Atlantic Ocean. *Journal of Micropaleontology*, 34, 21–49.
- Yasuhara, M., Okahashi, H., & Cronin, T. M. (2009). Taxonomy of Quaternary deep-sea ostracods from the Western North Atlantic Ocean. *Palaeontology*, 52, 879–931.
- Yasuhara, M., Okahashi, H., Cronin, T. M., Rasmussen, T. L., & Hunt, G. (2014). Response of deep-sea biodiversity to abrupt deglacial and Holocene climate changes in the North Atlantic Ocean. *Global Ecology and Biogeography*, 23, 957–967.
- Yasuhara, M., Stepanova, A. Y., Okahashi, H., Cronin, T. M., & Brouwers, E. M. (2014). Taxonomic revision of deep-sea Ostracoda from the Arctic Ocean. *Micropaleontology*, 60, 399–444.
- Yasuhara, M., Tittensor, D. P., Hillebrand, H., & Worm, B. (2015). Combining marine macroecology and paleoecology in understanding biodiversity: Microfossils as a model. *Biological Reviews*, 92, 199–215.
- Yin, Q., & Berger, A. (2010). Insolation and CO₂ contribution to the interglacial climate before and after the Mid-Brunhes Event. *Nature Geoscience*, 3, 243–246.
- Zarikian, A. C. A., Nadiri, C., Alonso-García, M., Rodrigues, T., Huang, H.-H. M., Lindhorst, S., Kunkelova, T., Kroon, D., Betzler, C., &

Yasuhara, M. (2022). Ostracod response to monsoon and OMZ variability over the past 1.2 Myr. *Marine Micropaleontology*, 102105. <https://doi.org/10.1016/j.marmicro.2022.102105>

BIOSKETCH

Anna B. Jöst is currently working as post-doctoral researcher at the Tropical and Subtropical Research Center of the Korea Institute of Ocean Science and Technology (KIOST) on Jeju Island, Republic of Korea. Her main focus of research are the controlling factors of spatial and temporal patterns of marine biodiversity and abundance distribution, and the role of anthropogenic disturbances and ecological processes in shaping these patterns, from deep-sea to shallow marine environments.

SUPPORTING INFORMATION

Additional supporting information can be found online in the Supporting Information section at the end of this article.

How to cite this article: Jöst, A. B., Huang, H.-H., Hong, Y., Wei, C.-L., Bauch, H. A., Thibodeau, B., Cronin, T. M., Okahashi, H., & Yasuhara, M. (2024). Testing the deep-sea glacial disturbance hypothesis as a cause of low, present-day Norwegian Sea diversity and resulting steep latitudinal diversity gradient, using fossil records. *Global Ecology and Biogeography*, 00, e13844. <https://doi.org/10.1111/geb.13844>